



Khaki, M., Forootan, E., Kuhn, M., Awange, J., van Dijk, A. I. J. M., Schumacher, M., & Sharifi, M. A. (2018). Determining water storage depletion within Iran by assimilating GRACE data into the W3RA hydrological model. *Advances in Water Resources*, 114, 1-18.  
<https://doi.org/10.1016/j.advwatres.2018.02.008>

Peer reviewed version

License (if available):  
Unspecified

Link to published version (if available):  
[10.1016/j.advwatres.2018.02.008](https://doi.org/10.1016/j.advwatres.2018.02.008)

[Link to publication record on the Bristol Research Portal](#)  
PDF-document

This is the author accepted manuscript (AAM). The final published version (version of record) is available online via Elsevier at <https://www.sciencedirect.com/science/article/pii/S0309170817306322?via%3Dihub#!> . Please refer to any applicable terms of use of the publisher.

## University of Bristol – Bristol Research Portal

### General rights

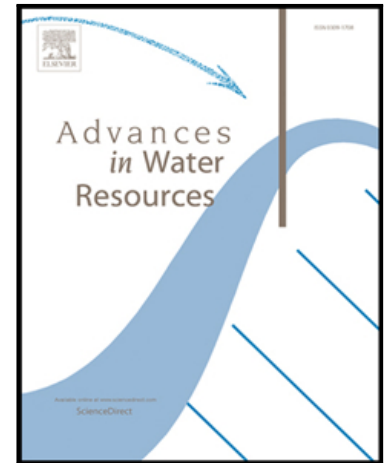
This document is made available in accordance with publisher policies. Please cite only the published version using the reference above. Full terms of use are available:  
<http://www.bristol.ac.uk/red/research-policy/pure/user-guides/brp-terms/>

## Accepted Manuscript

Determining Water Storage Depletion within Iran by Assimilating GRACE data into the W3RA Hydrological Model

M. Khaki, E. Forootan, M. Kuhn, J. Awange, A.I.J.M. van Dijk, M. Schumacher, M.A. Sharifi

PII: S0309-1708(17)30632-2  
DOI: [10.1016/j.advwatres.2018.02.008](https://doi.org/10.1016/j.advwatres.2018.02.008)  
Reference: ADWR 3094



To appear in: *Advances in Water Resources*

Received date: 19 June 2017  
Revised date: 1 February 2018  
Accepted date: 7 February 2018

Please cite this article as: M. Khaki, E. Forootan, M. Kuhn, J. Awange, A.I.J.M. van Dijk, M. Schumacher, M.A. Sharifi, Determining Water Storage Depletion within Iran by Assimilating GRACE data into the W3RA Hydrological Model, *Advances in Water Resources* (2018), doi: [10.1016/j.advwatres.2018.02.008](https://doi.org/10.1016/j.advwatres.2018.02.008)

This is a PDF file of an unedited manuscript that has been accepted for publication. As a service to our customers we are providing this early version of the manuscript. The manuscript will undergo copyediting, typesetting, and review of the resulting proof before it is published in its final form. Please note that during the production process errors may be discovered which could affect the content, and all legal disclaimers that apply to the journal pertain.

**Highlights**

- We assimilate GRACE data to improve a hydrological model estimations over Iran
- Ensemble Square-Root Filter is used for data assimilation
- We estimate sub-surface water storage changes within the country
- Climate and anthropogenic impacts on the water storages are investigated
- Independent in-situ measurements are used to evaluate the results

ACCEPTED MANUSCRIPT

# Determining Water Storage Depletion within Iran by Assimilating GRACE data into the W3RA Hydrological Model

M. Khaki<sup>a,1</sup>, E. Forootan<sup>b</sup>, M. Kuhn<sup>a</sup>, J. Awange<sup>a</sup>, A. I. J. M. van Dijk<sup>c</sup>, M. Schumacher<sup>d</sup>, M. A. Sharifi<sup>e,f</sup>

<sup>a</sup>*School of Earth and Planetary Sciences, Discipline of Spatial Sciences, Curtin University, Perth, Australia.*

<sup>b</sup>*School of Earth and Ocean Sciences, Cardiff University, Cardiff, UK.*

<sup>c</sup>*Fenner School of Environment and Society, the Australian National University, Canberra, Australia.*

<sup>d</sup>*School of Geographical Sciences, University of Bristol, Bristol, UK.*

<sup>e</sup>*Faculty of Surveying and Geospatial Engineering, College of Engineering, University of Tehran, Iran.*

<sup>f</sup>*Research Institute of Geoinformation Technology (RIGT), College of Engineering, University of Tehran, Iran.*

---

## Abstract

1 Groundwater depletion, due to both unsustainable water use and a decrease in precipitation, has  
 2 been reported in many parts of Iran. In order to analyze these changes during the recent decade,  
 3 in this study, we assimilate Terrestrial Water Storage (TWS) data from the Gravity Recovery  
 4 And Climate Experiment (GRACE) into the World-Wide Water Resources Assessment (W3RA)  
 5 model. This assimilation improves model derived water storage simulations by introducing  
 6 missing trends and correcting the amplitude and phase of seasonal water storage variations. The  
 7 Ensemble Square-Root Filter (EnSRF) technique is applied, which showed stable performance in  
 8 propagating errors during the assimilation period (2002-2012). Our focus is on sub-surface water  
 9 storage changes including groundwater and soil moisture variations within six major drainage  
 10 divisions covering the whole Iran including its eastern part (East), Caspian Sea, Centre, Sarakhs,  
 11 Persian Gulf and Oman Sea, and Lake Urmia. Results indicate an average of -8.9 mm/year  
 12 groundwater reduction within Iran during the period 2002 to 2012. A similar decrease is  
 13 also observed in soil moisture storage especially after 2005. We further apply the canonical  
 14 correlation analysis (CCA) technique to relate sub-surface water storage changes to climate  
 15 (e.g., precipitation) and anthropogenic (e.g., farming) impacts. Results indicate an average  
 16 correlation of 0.81 between rainfall and groundwater variations and also a large impact of  
 17 anthropogenic activities (mainly for irrigations) on Iran's water storage depletions.

*Keywords:* Iran, Groundwater Storage, Data Assimilation, Canonical Correlation Analysis, GRACE, W3RA Hydrological Model, Water Storage Depletion

---

*Email address:* Mehdi.Khaki@postgrad.curtin.edu.au (M. Khaki)

<sup>1</sup>Contact details: Department of Spatial Sciences, Curtin University, Perth, Australia, Email: Mehdi.Khaki@postgrad.curtin.edu.au, Tel: 0061410620379

## 18 1. Introduction

19 Water scarcity has become a serious issue in the Islamic Republic of Iran (abbreviated  
20 here as Iran) in recent years (e.g., [Amery and Wolf, 2000](#); [Wolf and Newton, 2007](#); [Trigo  
21 et al., 2010](#); [Madani, 2014](#); [Michel, 2017](#)). With the increased extraction of groundwater, its  
22 level has been reported to fall significantly (see, e.g., [Sarraf et al., 2005](#); [Motagh et al., 2008](#);  
23 [Mohammadi-Ghaleni and Ebrahimi, 2011](#); [Van Camp et al., 2012](#); [Afshar et al., 2016](#)). There  
24 have been studies that investigate surface and groundwater changes in Iran during the last  
25 decade (2003 onward) mainly using Terrestrial Water Storage (TWS) data from the Gravity  
26 Recovery And Climate Experiment (GRACE, [Tapley et al., 2004](#)). For example, [Voss et al.  
27 \(2013\)](#) reported  $\sim 143.6 \text{ km}^3$  reduction of freshwater from 2003 to 2009 over the north-central  
28 area of the Middle East, which largely covers the Tigris-Euphrates Basin. [Forootan et al.  
29 \(2014a\)](#) applied a statistical inversion to separate GRACE TWS using hydrological model out-  
30 puts and altimetry data as a priori information, and found a decrease in water storage with  
31 an average linear rate of  $\sim -15 \text{ mm/year}$  between 2002 and 2011. A large negative trend (2003-  
32 2012) in TWS was observed by [Joodaki et al. \(2014\)](#) using GRACE TWS data over the western  
33 Iran and eastern Iraq.

34 Estimating sub-surface water storages is very important since they support the life in semi-  
35 arid areas like Iran. [Fatolazadeh et al. \(2016\)](#) used the wavelet approach to improve estimates of  
36 groundwater storage variations from GRACE and found a remarkable decrease in groundwater  
37 in 2008, 2010 and particularly in 2011. [Forootan et al. \(2017\)](#) compared changes in water  
38 storage and hydrological water fluxes in Iran using GRACE and climate reanalysis data. Their  
39 results indicated that the decline of TWS in the Urmia and Tigris-Euphrates basins are greater  
40 than the decrease in the monthly accumulated total water fluxes. Therefore, it was concluded  
41 that the anthropogenic contribution on surface and groundwater flow is significant, and results  
42 in the storage decline within Iran.

43 These studies have proved the effectiveness of GRACE to enhance the understanding of  
44 water storage changes within the country. However, they do not provide a full understanding of  
45 spatially distributed water resources changes in different water compartments in Iran. GRACE  
46 TWS measures the summation of all water masses in the surface and sub-surface compart-  
47 ment of the terrestrial water storage (vegetation, snow, surface waters, soil, groundwater, etc.).  
48 Therefore, GRACE TWS must be separated into different storage compartments, which has  
49 been achieved to date through a forward modeling or an inversion framework as is described in

50 Forootan et al. (2014a) and the literature mentioned before.

51 To complement previous attempts, the aims of this study are to (i) update hydrological  
52 model simulations of sub-surface water storage changes (including water stored in the soil  
53 and groundwater storage) within Iran using GRACE data assimilation, and (ii) investigate  
54 climate and anthropogenic impacts on the estimated sub-surface water storages in (i). This  
55 study is the first data assimilation attempt to integrate GRACE TWS into the World-Wide  
56 Water Resources Assessment (W3RA; van Dijk, 2010) hydrological model over Iran. This  
57 methodology has been implemented in studies to constrain the mass balance of hydrological  
58 models over different river basins (e.g., Zaitchik et al., 2008; van Dijk et al., 2014; Eicker et al.,  
59 2014; Reager et al., 2015; Giroto et al., 2016; Schumacher et al., 2016). The main rationale in  
60 following this approach is that one relies on the physical processes, implemented in the model  
61 equations, to separate GRACE TWS into water compartments (see similar arguments, e.g., in  
62 Bertino et al., 2003). Thus, by generating ensemble members for a model derived water storage  
63 simulation, we will compute a priori estimates of mass redistribution in the country. Then,  
64 by assimilating GRACE data, while considering their uncertainty, we update (correct) these  
65 model estimations. A similar concept has also been followed in studies in hydrology, climate,  
66 and oceanography (see, e.g., Garner et al., 1999; Bennett, 2002; Kalnay, 2003; Schunk et al.,  
67 2004; Lahoz et al., 2007; Khaki et al., 2017a,b). In addition, by applying data assimilation, we  
68 will likely be able to reliably separate GRACE TWS data into different water compartments  
69 since both model and observation errors are considered. Considering that the spatial resolution  
70 of models is usually better than GRACE data, through the assimilation procedure, GRACE  
71 observations are downscaled, and therefore, higher resolution estimations of water storages will  
72 be available within the country (see also Schumacher et al., 2016; Khaki et al., 2018a).

73 Once improved model simulations are obtained, by assimilating GRACE TWS, relation-  
74 ships between the model-derived groundwater and soil moisture storages and climatic variables  
75 within Iran are investigated. To investigate the impacts of climate on the regional water stor-  
76 age estimates, precipitation from satellite remote sensing, temperature, and vegetation changes  
77 through the Normalized Difference Vegetation Index (NDVI) are used. Furthermore, anthro-  
78 pogenic effects are explored using the changes in water use for farming, industry, and human  
79 consumption. To this end, Canonical Correlation Analysis (CCA) is applied to provide an  
80 insight into the relations between model-derived water storages and both climatic and anthro-  
81 pogenic impacts by extracting spatio-temporal correlations between these inter-related data

sets. For a better spatial analysis of water storage and to reduce the uncertainty of estimations, the study area is divided into six major areas: the eastern part of Iran (indicated by East), Caspian Sea, Centre, Sarakhs, Persian Gulf and Oman Sea, and Lake Urmia (Figure 1).

The remainder of this study is structured as follows: Section 2 provides details on W3RA model, remotely sensed datasets, and in-situ measurements used. In Section 3, data assimilation filtering techniques, CCA algorithm, and the outline of our experimental setup are described. Results are presented and discussed in Section 4 including the data assimilation performance and analyzing the relationship between the model estimations, rainfall and NDVI through CCA. Finally, the study is concluded in Section 5.

FIGURE 1

## 2. Study area and data

### 2.1. Iran

Located in an arid and semi-arid region, Iran experiences strong regional differences in climate (Figure 1). Subtropical conditions are dominant over the northern part, but 90% of the country has limited rainfall with extremely hot summers in the central and southern coastal regions (Golian et al., 2015). Much of the west to northwest of Iran is located in high plateaus and mountain ranges associated with strong temperature differences between winter and summer. By contrast, the centre to southern parts are warm (cf. Figure 1) for most of the year with mild winters and hot summers. Annual rainfall, the main source of freshwater in Iran, varies from 50 mm in the deserts to 2275 mm in the northern part of the country (FAO, 2009). Only a fraction of the country receives enough rainfall for agriculture. A growing use of irrigation for agricultural productions (Ardakani, 2009) and the increasing population (from ~55 million in 1990 to ~80 million in 2015 Karamouzian and Haghdoost, 2015), make water availability an important issue across the country (Michel, 2017).

### 2.2. W3RA hydrological model

The present study uses the globally distributed World-Wide Water Resources Assessment system (W3RA) model, run at  $1^\circ \times 1^\circ$ . W3RA, based on the Australian Water Resources Assessment system (AWRA) model (version 0.5) developed in 2008 by the Commonwealth Scientific and Industrial Research Organization (CSIRO) is a daily grid-distributed biophysical

110 model that simulates landscape water stored in the vegetation and soil systems (see details in  
111 [van Dijk, 2010](#)). The model represent and forecast terrestrial water cycles ([van Dijk, 2010](#); [Ren-](#)  
112 [zullo et al., 2014](#)). W3RA does not consider anthropogenic effects (e.g., irrigation). Therefore,  
113 by assimilating GRACE TWS, which integrates both natural and anthropogenic signals (e.g.,  
114 [Schumacher et al., 2018](#)), we hope to constrain the model's water storage simulations and in-  
115 troduce the missing variations. Meteorological forcing data that is used here are minimum and  
116 maximum temperature, down-welling short-wave radiation, and precipitation from the Prince-  
117 ton University ([Sheffield et al., 2006](#)). The model contains effective soil parameters, water  
118 holding capacity and soil evaporation, relating greenness and groundwater recession, and satu-  
119 rated area to catchment characteristics parameters ([van Dijk et al., 2013](#)). This one-dimensional  
120 grid-based water balance model represents the water balance of the soil, groundwater and sur-  
121 face water stores in which each cell is modeled independently of its neighbors ([van Dijk, 2010](#);  
122 [Renzullo et al., 2014](#)). The model state, which is used for data assimilation (2002-2012), is com-  
123 posed of W3RA storages of the top, shallow root and deep root soil layers, and groundwater  
124 storage in an one-dimensional system (vertical variability).

### 125 *2.2.1. Satellite-derived observations*

126 We use monthly GRACE level 2 (L2) gravitational Stokes' coefficients truncated up  
127 to spherical harmonic degree and order 90 along with their full error information from 2002  
128 to 2012 provided by the ITSG-Grace2016 gravity field model ([Mayer-Gürr et al., 2014](#)). The  
129 monthly full error information of the Stokes' coefficients is used to construct an observation error  
130 covariance matrix for the GRACE TWS fields to be used for data assimilation ([Schumacher et](#)  
131 [al., 2016](#)). Degree 1 of Stokes' coefficients are replaced with those estimated by [Swenson et al.](#)  
132 (2008) to account for the movement of the Earth's center of mass. Degree 2 and order 0 (C20)  
133 coefficients are replaced by those from Satellite Laser Ranging solutions due to unquantified  
134 large uncertainties in this term (e.g., [Cheng and Tapley, 2004](#); [Chen et al., 2007](#)). Afterward,  
135 following [Wahr et al. \(1998\)](#), the L2 gravity fields is converted to gridded TWS fields with a  
136  $1^\circ \times 1^\circ$  spatial resolution.

137 Correlated noise in data due to anisotropic spatial sampling, instrumental noise (K-band  
138 ranging system and GPS), and temporal aliasing caused by the incomplete reduction of short-  
139 term mass variations ([Forootan et al., 2014b](#)) can be reduced by smoothing filters (e.g., [Kusche](#)  
140 [et al., 2009](#)). The application of smoothing, however, causes a spatial leakage problem that can



141 be problematic given that strong water resources of Tigris River and the Persian Gulf Basin can  
142 affect GRACE signals, as leakage-in errors, over the northwest and south of Iran, respectively.  
143 To tackle these errors, we use a Kernel Fourier Integration (KeFIn) filter, proposed by [Khaki](#)  
144 [et al. \(2018b\)](#), which defines an efficient averaging kernel to improve GRACE TWS within  
145 Iran. The KeFIn filtering method accounts for signal attenuations and leakage effects caused  
146 by smoothing in a two step filtering scheme (see more details in [Khaki et al., 2018b](#)). Lastly,  
147 in order to reach absolute TWS estimates (similar to W3RA), the mean TWS for the study  
148 period is taken from W3RA and added to the GRACE TWS anomalies time series.

149 Furthermore, since W3RA does not simulate lake dynamics, one needs to account for the  
150 existing surface water storage over the Lake Urmia before assimilation of the GRACE TWS  
151 data. Water level height datasets from satellite radar altimetry of Jason-1 (260 cycles from  
152 2002 to 2008) and Jason-2 (165 cycles from 2008 to 2012) are used to separate groundwater  
153 and surface water storage from GRACE TWS (more details in Section 3.1.2). We use the ExtR  
154 post-processing technique ([Khaki et al., 2014, 2015](#)) to retrack the data and improve water  
155 level measurements, which are erroneous within inland waters. Filtered surface heights are  
156 then used to create time series for virtual gauge stations over the Lake Urmia. These time  
157 series are subsequently used to remove the contribution of surface water storage changes from  
158 GRACE TWS data before implementing the proposed data assimilation (see also the procedure  
159 in [Forootan et al., 2014a](#)).

160 Satellite-derived precipitation data of TRMM-3B43 products ([TRMM, 2011](#)) from the Trop-  
161 ical Rainfall Measuring Mission Project (TRMM; version 7) is used to study rainfall variations.  
162 We convert the gridded precipitation products provided with a  $0.25^\circ \times 0.25^\circ$  spatial scale to  
163  $1^\circ \times 1^\circ$  for the period between 2002 and 2012. In addition, we use Version 4 gridded daily  
164 Normalized Difference Vegetation Index (NDVI) derived from the NOAA Climate Data Record  
165 (CDR) between 2002 and 2012 to further investigate climatic impacts. This dataset is pro-  
166 duced by the NASA Goddard Space Flight Center (GSFC) and the University of Maryland  
167 with a  $0.05^\circ \times 0.05^\circ$  spatial resolution. The datasets are rescaled to a  $1^\circ \times 1^\circ$  spatial resolution.  
168 A summary of the data sets and links to download the data are provided in Table 1.

### 169 2.2.2. Temperature

170 Monthly average temperature data for the temporal period of 2003 to 2012 is acquired  
171 from Climatic Research Unit (CRU; [Harris, 2008](#)), which is used in CCA as a climate indicator.

172 This data is provided using more than 4000 weather stations distributed around the world.  
173 For the sake of consistency with other data sets, the collected  $0.5^{\circ}\times 0.5^{\circ}$  spatial scale data is  
174 converted to  $1^{\circ}\times 1^{\circ}$ .

### 175 *2.3. In-situ data*

176 We use in-situ groundwater level data collected from 562 observation wells distributed  
177 over the six drainage divisions of East, Caspian Sea, Centre, Sarakhs, Persian Gulf and Oman  
178 Sea, and Lake Urmia water (cf. Figures 1) to compare them with our results. Datasets are  
179 provided by the Iran Water Resources Management Company (IWRMC) and are categorized  
180 based on Iran's six largest provinces on a yearly temporal scale presenting groundwater storage  
181 changes for an entire aquifer (Forootan et al., 2014a). Figure 2 shows an annual increase in  
182 groundwater extraction and the number of drilled wells for the entire country derived from  
183 IWRMC data sets. The IWRMC volumetric groundwater change measurements are converted  
184 to equivalent water height using the area of each aquifer. The area-averaged time series of  
185 groundwater changes for each aquifer is then generated and used for evaluating the results. The  
186 modified in-situ groundwater time series are compared separately to the average assimilation  
187 results for the same aquifer. River water discharge, the number of bore holes, and average  
188 water use for farming, industry, and urban use provided by IWRMC are also used in the CCA  
189 process (see Section 3.2). Details of all the applied datasets, as well as the model are presented  
190 in Table 1.

191 FIGURE 2

TABLE 1

## 192 **3. Method**

### 193 *3.1. Data assimilation*

#### 194 *3.1.1. EnSRF filtering*

195 In order to assimilate GRACE data into the W3RA model, we use the Ensemble Square-  
196 Root Filter (EnSRF) following Whitaker and Hamill (2002). EnSRF is an extended version  
197 of traditional Ensemble Kalman Filter (EnKF) that does not require the observations to be  
198 perturbed by introducing a new sampling scheme. Here, EnSRF is selected to avoid sampling

199 errors that can be reflected in the background covariance matrix especially in using a limited  
 200 number of ensembles (Whitaker and Hamill, 2002). Khaki et al. (2017a) showed that this  
 201 method is highly capable of assimilating GRACE TWS data into a hydrological model amongst  
 202 the most commonly used filters. EnSRF adopts a similar analysis step to the EnKF in the sense  
 203 that the analysis perturbations are computed from the forecast perturbations by updating each  
 204 ensemble perturbation with a Kalman-like update step. In the present study  $X$  consists of six  
 205 different water storages including top soil, shallow soil, and deep soil water, vegetation, snow,  
 206 and groundwater storages. Previous studies, e.g., Forootan et al. (2014a) and Tourian et al.  
 207 (2015), have investigated the surface water variations, specifically, in the Lake Urmia Basin  
 208 and the Caspian Sea as the major source of surface water storage changes in Iran. Therefore,  
 209 here, we only focus on the estimation of sub-surface compartments including groundwater and  
 210 soil moisture. The modified GRACE TWS data (see Section 2.2.1 for details) is then used to  
 211 update the above water compartments excluding surface storage.

212 The forecast model state, the integrated model state by a dynamical model for  $N$  times ( $N$   
 213 is the ensemble number), is represented by  $X^f = [X_1^f \dots X_N^f]$ , where  $X_i^f$  ( $i = 1 \dots N$ ) is the  
 214  $i$ th ensemble (hereafter ‘f’ refers to forecast and ‘a’ represents analysis). The corresponding  
 215 model state forecast error covariance of  $P^f$  is defined by:

$$P^f = \frac{1}{N-1} \sum_{i=1}^N (X_i^f - \bar{X}^f)(X_i^f - \bar{X}^f)^T, \quad (1)$$

$$\bar{X}^f = \frac{1}{N} \sum_{i=1}^N (X_i). \quad (2)$$

216 The update stage in EnSRF contains two steps. First, it updates the ensemble-mean following,

$$\bar{X}^a = \bar{X}^f + K(y - H\bar{X}^f), \quad i = 1 \dots N, \quad (3)$$

$$K = P^f(H)^T(HP^f(H)^T + R)^{-1}, \quad (4)$$

217 where  $K$  is the Kalman gain,  $y$  is the observation vector. The transition matrix and the  
 218 observation covariance matrix are indicated by  $H$  and  $R$ , respectively. Next, EnSRF updates  
 219 the forecast ensemble of anomalies  $A^f = [A_1^f \dots A_N^f]$  into the analysis ensemble deviation  $A^a$ .  
 220  $A^f$  as the deviation of model state ensembles from the ensemble mean is derived from,

$$A_i^f = X_i^f - \bar{X}^f. \quad (5)$$

221 EnSRF exploits the serial formulation of the Kalman filter analysis step in which the observa-  
 222 tions are assimilated each at a time to compute the analysis perturbations that exactly match  
 223 the Kalman filter covariance (Hoteit et al., 2008) using the modified gain ( $\tilde{K}$ ) with,

224

$$A^a = (I - \tilde{K}H)A_i^f, \quad (6)$$

$$\alpha = \left(1 + \sqrt{\frac{R}{HP^fH^T + R}}\right)^{-1}, \quad (7)$$

225 where  $I$  is an identity matrix. More details on EnSRF can be found in Whitaker and Hamill  
 226 (2002) and Tippett et al. (2003).

### 227 3.1.2. Assimilating GRACE TWS into W3RA

228 Monthly gridded GRACE TWS data are assimilated into W3RA to update the model  
 229 states, a summation of model vertical water compartments (here soil moisture, vegetation  
 230 biomass, snow, and groundwater). Note that no parameter adjustment is considered here  
 231 and the observations are only used to constrain the system states. The monthly increment (i.e.,  
 232 the difference between the monthly averaged GRACE TWS and simulated TWS) can be added  
 233 to each day of the current month, which guarantees that the update of the monthly mean is  
 234 identical to the monthly mean of the daily updates. In practice, the differences between the  
 235 predictions and the updated states are added as offsets to the state vectors at the last day of  
 236 each month to generate the ensembles for the next month assimilation step. We use Monte  
 237 Carlo sampling of multivariate normal distributions with the errors representing the standard  
 238 deviations of the forcing sets (precipitation, temperature, and radiation) to generate an ini-  
 239 tial ensemble (Renzullo et al., 2014). The perturbed meteorological forcing datasets, then, are  
 240 integrated forward with the model from 2000 to 2002 providing 72 sets of state vectors (as  
 241 suggested by Oke et al., 2008) at the beginning of the study period.

242 An application of small ensemble size is problematic in ensemble data assimilation systems,  
 243 as it can lead to filter divergent or inaccurate estimation (Tippett et al., 2003). Therefore,  
 244 we apply ensemble inflation that uses a small coefficient factor (here 1.12; Anderson et al.,  
 245 2001) to inflate prior ensemble deviation from the ensemble-mean and increases their variations  
 246 (Anderson et al., 2007). Furthermore, the Local Analysis (LA) scheme (Evensen, 2003; Ott et  
 247 al., 2004) is applied for localization. LA improves the assimilation procedure by restricting the

248 observations used for the covariance matrix computation to a spatially limited area (Khaki et al.,  
 249 2017c). As a result, only those measurements located within a certain distance from a grid point  
 250 have an impact on the updated states (Evensen, 2003; Ott et al., 2004). Different localization  
 251 lengths are tested and their results are assessed against in-situ groundwater measurements  
 252 (Section 2.3) to reach the best case scenario (i.e.,  $5^\circ$  half-width used in this study).

253 As mentioned, it is necessary to remove surface water storages from GRACE TWS data over  
 254 Lake Urmia before data assimilation. For this purpose, following Forootan et al. (2014a) who  
 255 undertook water analysis over the same area, we use satellite altimetry time series over the lake  
 256 to derive surface water storage. The Global Land Data Assimilation System (GLDAS) outputs  
 257 of total column soil moisture, snow water equivalent, and vegetation biomass water storage as  
 258 well as water level variations from altimetry are used to estimate temporal and spatial patterns  
 259 of surface water storage using Independent Component Analysis (ICA). The extracted patterns  
 260 are then adjusted to GRACE TWS products using a least squares adjustment (LSA) procedure  
 261 (see details in Forootan et al., 2014a). The GRACE data after removing surface water storage  
 262 is used for the data assimilation process over Lake Urmia.

### 263 3.2. Canonical Correlation Analysis (CCA)

264 The present study applies Canonical Correlation Analysis (CCA) to find the linear  
 265 connection of two sets of multidimensional variables of predictor ( $x_c$ ) and criterion ( $y_c$ ) values.  
 266 CCA is selected here rather than simple correlation analysis due to its ability in establishing  
 267 the relationships between multiple intercorrelated variables. CCA extracts canonical coefficients  
 268 that represent common processes between two or more variables (Chang et al., 2013) using an  
 269 eigenvector decomposition that yields linear weights, known as canonical coefficients, which  
 270 describe maximum correlations between variables (see details in Steiger and Browne, 1984).  
 271 The combination of variables with the first canonical coefficient for each set has the highest  
 272 possible multiple correlations with the variables in the other set. CCA extracts canonical  
 273 coefficients  $u$  and  $v$  such that  $X_c = x_c^T u$  and  $Y_c = y_c^T v$  ( $X_c$  and  $Y_c$  are canonical variates)

274 possess a maximum correlation coefficient (Chang et al., 2013) using the following function,

$$\begin{aligned}
 R &= \frac{E[X_c Y_c]}{\text{sqrt}(E[X_c^2] E[Y_c^2])} \\
 &= \frac{E[u^T x_c y_c^T v]}{\text{sqrt}(E[u^T x_c x_c^T u] E[v^T y_c y_c^T v])} \\
 &= \frac{u^T C_{x_c, y_c} v}{\text{sqrt}(u^T C_{x_c, x_c} u v^T C_{y_c, y_c} v)},
 \end{aligned} \tag{8}$$

275 where  $C_{x_c, x_c}$  and  $C_{y_c, y_c}$  are covariance matrices of  $x_c$  and  $y_c$ , respectively and the objective in  
 276 above function is to maximize the correlation  $R$ . We use an eigenvalue decomposition procedure  
 277 to find the linear weights producing canonical coefficients, which imply maximum possible  
 278 correlations (see details in Steiger and Browne, 1984). There are different canonical coefficients  
 279 within each set leading to different uncorrelated coefficients. Nevertheless, the combination  
 280 of variables with the first canonical coefficient for each set has the highest possible multiple  
 281 correlations with the variables in the other set.

282 Two scenarios are considered for prediction: (i) the predictor ( $x_c$ ) contains time series  
 283 of both groundwater used for farming, industry, and human consumption from IWRMC and  
 284 climate-related variables of precipitation, NDVI, and temperature (provided by Harris, 2008),  
 285 and (ii) the predictor ( $x_c$ ) includes only climate-related variables of precipitation, NDVI, and  
 286 temperature. This is done to explore the impact of each scenario on water variations. The  
 287 criterion ( $y_c$ ) in both scenarios contains water storage (groundwater and soil moisture) and  
 288 discharge (from IWRMC) variations. By applying CCA, we establish the best combinations  
 289 between two sets of variables in two different cases. By comparing the results of these two  
 290 scenarios, we can investigate how water use and climate variabilities impact water storage  
 291 changes within Iran. Nevertheless, there are other effective components (e.g., large-scale ocean-  
 292 atmosphere phenomenon, evaporation, and droughts) on the water storage, which is difficult to  
 293 include all of them in the process. This CCA scheme, however, could provide an insight on the  
 294 connection between the above components. Table 2 summarizes the experiments undertaken  
 295 in this study. The corresponding research objectives and related sections that contain each  
 296 experiment's results are also listed in the table.

TABLE 2

## 297 4. Results and discussion

### 298 4.1. Simulated assimilation

299 In the following, we analyze the effect of various scenarios of observations on the as-  
300 simulation. As mentioned earlier, GRACE TWS observations are used to update the sum of  
301 soil moisture, vegetation, snow, and groundwater compartments at each grid cell. Thus, it is  
302 important to investigate the distribution of the increments between these compartments, espe-  
303 cially soil moisture and groundwater storage while the influence of the remaining storages (i.e.,  
304 vegetation and snow) is negligible. In particular, we are interested in monitoring the impacts  
305 of trends in observations time series on different water components. [Schumacher et al. \(2018\)](#)  
306 showed that assimilating GRACE TWS data can improve model simulation of seasonality and  
307 trend of TWS, as well as individual water storage components. This point is important be-  
308 cause the largest part of GRACE TWS trends caused by groundwater variations that originate  
309 from both natural and human-induced (e.g. water use) changes while soil moisture variations  
310 generally follow climate pattern. Simulation experiments are undertaken to monitor how obser-  
311 vations' variations, and particularly their trends are reflected in soil moisture and groundwater  
312 estimates during assimilation.

313 To illustrate how GRACE data assimilation can improve model states, we perform a syn-  
314 thetic study, in which arbitrary errors (uncertainty with different magnitudes) are assigned to  
315 different model derived water storage states. We evaluate whether these states accurately re-  
316 ceive increments from GRACE TWS. To this end, we introduce different uncertainties to model  
317 states and test how these are transferred to the assimilation forecast steps (cf. Eqs. (3)-(4)).  
318 Figure 3 shows the relationship between selected uncertainties of water states and their corre-  
319 sponding weights in the (synthetic) assimilation. Based on this setup, six different scenarios are  
320 considered to explore the impact of weights as the ratio of the assigned increment derived for  
321 each storage state to the summation of all states. The results presented in Figure 3 indicate an  
322 average influence of assimilating GRACE TWS data into W3RA over Iran between 2003 and  
323 2013. In general, as theoretically expected, higher weight (i.e., larger increment) is assigned  
324 to a variable with a smaller uncertainty. In other words, by assimilating GRACE TWS, the  
325 model's water states with larger uncertainty receive larger increments, and this is reverse for  
326 states with smaller uncertainty. These results approve the recent results of [Schumacher et al.](#)  
327 (2018), who assimilate GRACE TWS data into WGHM model over Australia. Figure 3 also  
328 shows that the average correlations between the individual estimated storage in each scenario

329 and the assimilated GRACE TWS. The correlations are calculated after removing seasonal ef-  
330 fects on time series to focus on trends. It can be seen that larger correlations to the GRACE  
331 TWS trends are obtained for a compartment with larger uncertainty and correspondingly with  
332 a larger increment. This means that the assimilation process transfers the observation trends  
333 into the more uncertain storage, which receives the larger corrections.

FIGURE 3

334 Another synthetic experiment is also implemented, where, different observation sets are  
335 assimilated into W3RA but this time without manipulating their uncertainties. The aim is to  
336 investigate whether the distribution of increments of different water states changes when the  
337 TWS observations change. Here, four different synthetic observation scenarios are considered,  
338 which include two versions of the WaterGAP Global Hydrology Model (WGHM; more details  
339 on [Döll et al., 2003](#); [Müller et al., 2014](#)) TWS estimates with and without water abstractions,  
340 GRACE-derived TWS, and GRACE TWS minus WGHM soil moisture that roughly gives  
341 groundwater observations. The spatially averaged time series of the TWS observations (for the  
342 first three cases) over Iran are displayed in Figure 4a. The difference between the WGHM TWS  
343 observations with and without water use clearly show the anthropogenic impacts as a distinct  
344 negative trend in WGHM with water abstraction impact. A similar trend can also be seen in  
345 GRACE TWS. Assimilation of these observations can show how water storages, for example  
346 their trends, are distributed between soil moisture and groundwater estimates. Assimilating  
347 WGHM TWS without water use, which does not show any significant trends, might better  
348 estimate soil moisture. This is due to the fact that the main source of TWS's negative trends is  
349 groundwater exploitation, while soil moisture variations generally are related to climatic (e.g.,  
350 precipitation) variations. Hence, comparing the soil moisture results of assimilating GRACE  
351 TWS and WGHM TWS with water use with those of WGHM TWS without water use can help  
352 to assess the performance of data assimilation in updating soil moisture. Furthermore, while  
353 the first three observation sets (i.e., WGHM with and without water use and GRACE-derived  
354 TWS) are used to update the summation of all compartments, the last case (GRACE TWS  
355 minus WGHM soil moisture) is used to update only the groundwater simulations. The main  
356 rationale for updating only groundwater in the last experiment is to compare its results with  
357 the other scenarios, which can help to investigate how accurate groundwater corrections are



358 applied from TWS increments in the other cases, where different compartments are available.

#### FIGURE 4

359 The results of the data assimilation variants are shown in Figures 4b and 4c and updated  
 360 groundwater estimates from assimilating GRACE TWS minus WGHM soil moisture is plotted  
 361 in Figure 4c. The assimilation results for soil moisture (Figure 4b) and groundwater (Figure  
 362 4c) show that the negative TWS trends are largely reflected only in groundwater time series.  
 363 The average correlation between the above TWS observations and corresponding groundwater  
 364 estimates is 0.92, 42% (on average) larger than for the open-loop run, which indicates the  
 365 suitability of data assimilation for constraining system states. For the entire area, there is  
 366 a stronger agreement between the soil moisture from assimilation compared to the open-loop  
 367 run, e.g., 22% (on average) for the GRACE TWS case and 28% (on average) for the WGHM  
 368 TWS with water use case. Lower correlations are obtained for assimilating WGHM TWS  
 369 without water use in comparison to other data assimilation scenarios (see also Figure 4b).  
 370 Furthermore, groundwater variations from the assimilated GRACE TWS are largely correlated  
 371 to the groundwater estimates from assimilating only groundwater observations (GRACE TWS  
 372 minus WGHM soil moisture). TWS observations of WGHM without water use have the least  
 373 effect on groundwater variations.

374 It can be concluded from Figure 4 that the data assimilation process successfully distributes  
 375 TWS increments between soil moisture and groundwater storages. These results indicate that  
 376 the largest part of increments during data assimilation is assigned to groundwater. The larger  
 377 impact on groundwater, based on Figure 3, suggests that the groundwater estimation of W3RA  
 378 is more uncertain than its soil moisture and as a result it receive larger updates. This is even  
 379 more clear in Figure 5, where groundwater and soil moisture estimates by ensemble members be-  
 380 tween 2004 and 2008 are shown. This time period is selected because it includes an episode with  
 381 strongly negative groundwater trend after 2005 (see also Figure 4c), where ensemble spreads  
 382 show a different pattern, e.g., larger spreads. The propagated groundwater ensemble members  
 383 are more dispersed than those of soil moisture, which causes larger ensemble deviations from its  
 384 mean and consequently larger uncertainty for the states (cf. Eqs. (1)-(2)). This can be due to  
 385 the point that the W3RA model has a simplified simulation of groundwater dynamics for un-  
 386 confined groundwater and does not simulate confined groundwater dynamics or anthropogenic

387 groundwater extraction (Tregoning et al., 2012). The larger corrections applied to groundwater  
388 is also realistic considering the fact that a majority of water depletion in Iran occurs in ground-  
389 water due to large extractions for irrigation. The applied irrigation water is likely to locally  
390 increase total soil column water storage, which may contribute to a smaller decline in soil water  
391 content (Michel, 2017).

FIGURE 5

392 Even though the results indicate good performance of GRACE data assimilation, one might  
393 still expect artefacts from the TWS increments on the state estimates. The absence of ground-  
394 water abstractions and anthropogenic impacts in most hydrological models, especially where  
395 the rate of this extraction is high, can cause a misinterpretation of a negative TWS trend  
396 captured by GRACE in the system states. As shown by Giroto et al. (2017), the assimila-  
397 tion of GRACE TWS can successfully introduce the negative trends in the modeled TWS and  
398 groundwater, however, this can also introduce unrealistic decline in other components, e.g., soil  
399 moisture and evapotranspiration. This effect can be exacerbated when groundwater extraction  
400 is large and occurs over an extended period. The model dynamical range of groundwater may  
401 not be sufficient to accommodate the assimilated values (Zaitchik et al., 2008; Li and Rodell,  
402 2015). Despite these, merging GRACE TWS data with high resolution models is the most ef-  
403 ficient existing approach to analyze groundwater changes over wide areas, which in most cases  
404 results in an improvement in the estimates (Li and Rodell, 2015; Giroto et al., 2017). Here,  
405 we addressed this challenge by conducting a synthetic experiment, as well as by independently  
406 assessing groundwater and soil moisture from assimilation. However, more investigations are  
407 needed to be extended and the impacts of various data assimilation scenarios on each individual  
408 water compartments need to be tested. These investigations are, however, out of the scope of  
409 this study.

#### 410 4.2. Result evaluation

411 In this section, we assess the performance of data assimilation using in-situ groundwater  
412 measurements. To examine the validity of data assimilation results, in-situ groundwater mea-  
413 surements of the six major drainage regions in the area including the East, Caspian Sea, Centre,  
414 Sarakhs, Persian Gulf and Oman Sea, and Lake Urmia (cf. Figure 1) are used. For each basin in  
415 Figure 1, we calculate the spatial average time series of groundwater storages with and without

416 data assimilation and compare them with the IWRMC in-situ and WGHM groundwater varia-  
 417 tion. We first analyze the performance of two assimilation cases of GRACE TWS and GRACE  
 418 TWS minus WGHM soil moisture data assimilation experiments for improving groundwater  
 419 estimates. Figure 6 shows the average root-mean-square error (RMSE) and standard deviation  
 420 (STD) calculated using groundwater from assimilation cases and in-situ measurements. Both  
 421 cases perform comparably in terms of RMSE and STD with an average of 38% error reduction  
 422 compared to open-loop. Nevertheless, assimilating GRACE TWS obtains the smaller RMSE  
 423 than groundwater only data assimilation. This further confirms the effectiveness of the applied  
 424 data assimilation for distribution TWS increments, especially for groundwater storage. Based  
 425 on this assessment, hereafter only the results for GRACE TWS data assimilation are presented.

FIGURE 6

426 The results for groundwater examination from data assimilation, WGHM, and the open-  
 427 loop run for each drainage division are illustrated in Figure 7, which show that the strongest  
 428 agreement between groundwater estimates and in-situ measurements occur in the assimilation  
 429 results. In most of the cases, WGHM performs better than the open-loop. For a better assess-  
 430 ment of data assimilation results, additional agreement statistics using RMSE and correlation  
 431 analysis are calculated and reported in Table 3. Significance at  $p < 0.05$  was calculated using  
 432 the Students t-test with consideration of temporal autocorrelation through effective sample size.

FIGURE 7

TABLE 3

433  
 434 The computed time series for each region is compared to IWRMC data for the corresponding  
 435 region in order to estimate the reported statistics in Table 3. Generally, the assimilation results  
 436 are largely correlated with the in-situ data (0.85 on average) after data assimilation, with an  
 437 improvement of 35% over open-loop results. The largest improvements in terms of correlation  
 438 increase and RMSE reduction with respect to the in-situ measurements are achieved over Lake  
 439 Urmia, Sarakhs, and to a lesser degree Persian Gulf and Oman Sea. Table 3 shows considerable  
 440 groundwater decline in most of the regions especially within the Persian Gulf and Oman Sea  
 441 and Lake Urmia (both mostly located in the western areas). The largest negative groundwater

442 trend is exhibited for Lake Urmia while the lowest trend is found for the Caspian Sea division  
 443 in the north, which could be attributed to a large amount of precipitation in the latter region.

444 We further examine the soil moisture estimates from data assimilation. In the absence  
 445 of reliable in-situ soil moisture measurements over the study area, we use satellite-derived  
 446 and independent model soil moisture products. Soil moisture observations from the Advanced  
 447 Microwave Scanning Radiometer - Earth Observing System (AMSR-E) and Soil Moisture and  
 448 Ocean Salinity (SMOS) are compared to the assimilated top layer soil moisture estimates. The  
 449 motivation behind this comparison is based on the fact that SMOS and AMSR-E measurements  
 450 are largely correlated, respectively, to surface 0-5 cm and 0-2 cm soil moisture content (Njoku  
 451 et al., 2003). Figure 8 shows the average time series of the above comparison within the  
 452 study period. It can be seen that the assimilation top layer soil moisture is better matched  
 453 (41% improvement in correlation) to the satellite measurements in comparison to the open-loop  
 454 estimates. This shows a successful impact of GRACE TWS data assimilation on the model top  
 455 layer.

FIGURE 8

456 Total soil moisture estimates from data assimilation, i.e., summation of soil moisture at top,  
 457 shallow- and deep-root layers, are compared with soil moisture estimates of WGHM, the Global  
 458 Land Data Assimilation System (GLDAS; Rodell et al., 2004), and soil moisture provided by van  
 459 Dijk et al. (2014), who combined different data (e.g., GRACE) and model outputs (indicated  
 460 here as W3). The results are displayed in Figure 9. In all cases, data assimilation leads to a  
 461 better agreement to other products with an average 25% improvement. The largest correlation,  
 462 as well as the greatest improvement, are found for soil moisture after assimilation of WGHM.  
 463 There is also a considerable correlation between the results and W3.

FIGURE 9

#### 464 4.3. *Water storage analysis*

465 Based on the improved soil moisture and groundwater estimates, spatio-temporal varia-  
 466 tions of both compartments are analyzed in this section. The variation of groundwater storages  
 467 within Iran before and after data assimilation are illustrated in Figure 10. The blue graph in  
 468 Figure 10 represents the average groundwater variations of all grid points after data assimi-

469 tion. This graph clearly shows a negative trend between 2002 and 2013 with an average -8.9  
 470 mm/year groundwater depletion for the entire country. However, such a trend is not present in  
 471 the open-loop time series. GRACE TWS data assimilation constrains groundwater estimates  
 472 and introduces this negative trend into the state as it exists in GRACE TWS observations (cf.  
 473 Figure 4). It is evident that the W3RA without data assimilation is not able to provide reli-  
 474 able long-term changes of groundwater, e.g., trend and multi-year variations. Therefore, data  
 475 assimilation is vital for reliable interpretation of ground water beyond the annual cycle. How-  
 476 ever, without additional information the data assimilation results cannot differentiate between  
 477 natural and anthropogenic causes. Apart from the trends, Figure 10 also shows a multi-year  
 478 cycle, e.g., positive trend between 2002 and 2005 and a stronger negative trend for the later  
 479 years 2006 to 2013. Again, this trend is not visible in the open-loop simulations.

FIGURE 10

480 Furthermore, we separately analyze water compartments for each of Iran's major drainage  
 481 regions. The soil moisture and groundwater average time series from W3RA before and after  
 482 assimilating GRACE TWS for each of the divisions are shown in Figure 11 and Figure 12,  
 483 respectively. Larger soil moisture variations (in terms of amplitude) exist for the data assimi-  
 484 lation results compared to open-loop results in Figure 11. In particular, this is evident for the  
 485 Persian Gulf and Oman Sea and Caspian Sea. This could be due to a larger amount of annual  
 486 precipitation over these areas. Declines in soil water content can be seen in Sarakhs, especially  
 487 between 2005 and 2009, and Lake Urmia. In most of the regions, increases (e.g., large positive  
 488 variations) are observed during 2004 and 2010. Overall, better agreements between open-loop  
 489 and assimilation time series are found over East and Centre regions, where a semi-arid cli-  
 490 mate condition is dominant. GRACE data assimilation has the least impact on soil moisture  
 491 estimates within these areas.

FIGURE 11

492 Figure 12 depicts groundwater variations for each individual drainage division. Similar to  
 493 soil moisture analysis (cf. Figure 11), data assimilation results demonstrate larger magnitudes  
 494 than open-loop results. Except for the Caspian Sea, all the regions show a considerable decline  
 495 in groundwater estimates during the study period. In particular, this is clear in Lake Urmia,

496 Sarakhs, and Centre, especially after 2007. These trends are absent in the open-loop time series  
 497 and derive from GRACE TWS after implementing data assimilation, which confirm the results  
 498 shown in Figure 10. Larger groundwater declines are found in regions over the western parts  
 499 of the country (e.g., the Persian Gulf and Oman Sea and Lake Urmia). In most of the cases,  
 500 groundwater rise is observed as a positive trend between 2004 and 2005. These increases are  
 501 then followed by consistent declines despite some short-term increases such as during 2010. A  
 502 large trend decline is observed after 2006 in Lake Urmia, Centre, Sarakhs, and to a lesser degree  
 503 in Caspian Sea. For the Persian Gulf and Oman Sea, Sarakhs, and Center, the groundwater  
 504 negative trend is remarkable after 2008. Despite a small negative trend in East for the study  
 505 period, the groundwater variations have the smallest amplitudes in this region compared to  
 506 other areas. Seasonal variations can clearly be seen in most of the regions while this pattern is  
 507 dominant mostly in Caspian Sea. Figure 12 and the reported negative trends in Table 3 show  
 508 that groundwater depletion is a major issue in most parts of Iran resulting in a remarkable  
 509 dryness across the country.

FIGURE 12

#### 510 4.4. Climatic impacts

511 We further investigate the connection between climatic impacts and water storage vari-  
 512 ations. A comparison between groundwater and soil moisture variations and climate-related  
 513 variables such as precipitation and NDVI can reveal such interactions these parameters. Figure  
 514 13 shows maps of temporal average precipitation, soil moisture, and groundwater maps during  
 515 the study period. The first row in Figure 13 represent the average applied increment to soil  
 516 moisture and groundwater storages, the second row indicates variations (average of time series  
 517 at each grid point) of precipitation, soil moisture, and groundwater, and trends for each variable  
 518 at each grid point are depicted in the third row.

FIGURE 13

519 Figure 13 shows the spatial pattern of increments, i.e., the difference between assimilation  
 520 results and open-loop estimates, applied to the system states. It can be seen that the largest  
 521 increments are applied to groundwater storage as can be expected from Figures 3 and 4. These  
 522 corrections are mostly focused on the northwest to south and the eastern part of Iran. In soil

523 moisture, the increments can be found across the country, again, with larger concentrations  
524 in the western areas. The effect of data assimilation clearly can be seen by the increments  
525 illustrated in Figure 13. The spatial pattern of precipitation, soil moisture, and groundwater  
526 variations in Figure 13 show larger variations over the north toward northwest parts, where the  
527 Alborz mountain range cover a large portion of the areas. A similar pattern can also be seen  
528 in western parts, where the Zagros mountain range is located. Overall, the soil moisture map  
529 more closely reflects the precipitation patterns compared to groundwater variations, which can  
530 be attributed to impacts from water uses. Contrary to precipitation and soil moisture, negative  
531 groundwater variations are found over different regions, especially the north-western and south-  
532 ern parts. There are very limited variations in terms of amplitude changes for precipitation,  
533 soil moisture, and groundwater within the centre, eastern, and partially south-eastern parts of  
534 Iran. Trend maps (last row in Figure 13) illustrate spatial patterns for each component. Both  
535 precipitation and soil moisture show increasing trends in the north and to a lesser degree in  
536 the south. Groundwater trends are generally negative in all regions, but more strongly in the  
537 west, where Lake Urmia is located. A significant groundwater depletion can be observed in  
538 the central parts extended to the north, where Tehran, Iran's capital city is located. Large  
539 groundwater extractions in Tehran during the study period can be the main reason for this  
540 while in other areas, an excessive irrigation is a potential candidate for the observed depletion.  
541 It can be seen that there is an agreement between the applied increment by data assimilation,  
542 especially for groundwater, and the negative observed trends. Again it can be concluded that  
543 without using assimilation, these negative trends are not captured.

544 To better quantify the spatio-temporal variations of water storage and climate variabilities,  
545 principal component analysis (PCA Lorenz, 1956) is applied on precipitation, NDVI, GRACE  
546 TWS, and groundwater time series. This allows us to monitor the relationship between the  
547 estimated groundwater and GRACE TWS, as well as their connection to climatic impacts  
548 through precipitation and NDVI. The first three extracted principal components (PC1, PC2,  
549 and PC3) of each component are plotted in Figure 14. There is good agreement between the  
550 time series for all three cases, in particular for seasonal variations. All time series in PC1  
551 show a clear annual variation. Negative trends, especially after 2009 are only captured by  
552 PC1 of GRACE TWS and groundwater. Stronger agreements between precipitation and NDVI  
553 PCs can be found. This can be attributed to vegetation growth response to rainfall and soil  
554 moisture. The assimilated groundwater storage variations largely follow the GRACE TWS

555 variation patterns, both in terms of variability and trend, mainly due to the application of  
556 GRACE data assimilation. Both of these variables are strongly correlated with rainfall time  
557 series in PC2 and PC3 with an average correlation of 0.86. Various strong anomalies are occur in  
558 the time series, e.g., in 2005 and 2010. Increases in the time series occur in PC1 for all variables  
559 between 2004 and 2006 and during 2010 and 2012. PC2 shows similar rises in 2008 and 2010  
560 followed by a strong decrease. PC3 shows an increase in 2009 and 2010 in the precipitation,  
561 GRACE TWS, and groundwater which explains the corresponding increase in water storages  
562 (cf. Figures 10 and 12). Some negative anomalies are found in PC3 in 2003, 2005, and 2011 and  
563 also in 2006 and 2013. The other variables generally demonstrate the same variation pattern as  
564 precipitation, which shows a strong connection between water storage variations and climatic  
565 changes. Water storage variations in Iran, however, are also affected by non-climate factors  
566 (e.g., anthropogenic impacts), which are likely the cause of the observed negative trends in  
567 PC1 for GRACE TWS and groundwater.

FIGURE 14

568 The corresponding empirical orthogonal functions (EOF1, EOF2, and EOF3) extracted by  
569 applying PCA on precipitation, NDVI, GRACE TWS, and groundwater from data assimilation  
570 are shown in Figure 15. Overall, the mode 1 represents a strong annual signal (as would be  
571 expected), mode 2 shows some deviations from the annual signal (e.g. inter-annual variations)  
572 in the same regions as for mode 1. Mode 3 to some extent shows inter-annual variations but  
573 importantly shows some extreme values. The spatial patterns of NDVI, GRACE TWS, and  
574 groundwater are largely correlated to rainfall pattern, especially in EOF1 and EOF2. Larger  
575 spatial variations exist over the northern and western parts of Iran, which seem to cause larger  
576 water storage and NDVI changes in the same areas. These are the parts with higher altitudes  
577 in which precipitation rates are generally high. GRACE TWS and groundwater EOF2 maps  
578 show strong positive signals over the north toward the northwest and partially in western areas.  
579 The rainfall EOF2 map, however, does not show a large signal over the north-western part but  
580 only over the northern and western parts, where the Alborz and Zagros mountain ranges are  
581 located. On the other hand, all variables show a negative signal in the south-eastern part.  
582 Positive signals over the eastern parts, with smaller amplitudes, compared to EOF1 and EOF2  
583 for NDVI, GRACE TWS, and groundwater are displayed by EOF3 maps. Negative signals can



584 be seen in EOF3 maps, especially for groundwater mostly over the northwestern areas, where  
 585 Lake Urmia is located, as well as the northeast and Sarakh.

FIGURE 15

#### 586 4.5. CCA results

587 We further implement CCA on the estimated water compartments (from the data as-  
 588 simulation) on the one hand, and human- as well as climate-related variables on the other hand  
 589 in two different scenarios, i.e., (i) the predictor contains time series of both groundwater used  
 590 (e.g., for farming and industry) and climate-related variables (precipitation, NDVI, and tem-  
 591 perature), and (ii) the predictor includes only climate-related variables of precipitation, NDVI,  
 592 and temperature (cf. Section 3.2). By this, we can establish the relations between water stor-  
 593 ages and other factors. CCA is applied to the spatially averaged time series of all variables  
 594 to estimate canonical coefficients. Canonical loadings are used to interpret the CCA results,  
 595 which measure the simple linear correlation between an observed variable and the estimated  
 596 canonical variates (Dattalo, 2014). The interpretation is mostly based on examining the sign  
 597 and the magnitude of the canonical coefficients assigned to each variable. Variables with larger  
 598 coefficients contribute more to the variates and variables with opposite signs exhibit an inverse  
 599 relationship with each other while those with the same sign exhibit a direct relationship. De-  
 600 tailed results of the CCA experiment for each scenario applied within Iran are presented in  
 601 Table 4.

TABLE 4

602 The table summarizes the contribution of each variable in CCA. Results indicate that sce-  
 603 nario (i) leads to larger canonical correlation coefficients in comparison to scenario (ii). This  
 604 means that variations in water storages are more correlated to variations of the combined  
 605 human- and climate-related parameters. Note that CCA extract different sets of results (roots),  
 606 thus, we only use the first root that is statistically significant (for a significant level of 0.05). It  
 607 can be seen from Table 4 that the water use has strong negative correlations to water storage  
 608 variations, especially groundwater, which has the largest loading. This means that water con-  
 609 sumption for various uses (especially farming) is a very effective factor within the country that  
 610 causes the greatest impact on groundwater (with 0.938 canonical correlation). Among climate

611 variables, precipitation, and to a lesser degree temperature have also a considerable influence  
612 on water storage variations. Not surprisingly, an increase (or decrease) in rainfall directly leads  
613 to increase (or decrease) in water storages as indicated by the same signs. Table 4 suggests that  
614 variations in groundwater use and climate parameters in both scenarios have minimum impact  
615 on water discharge. This may be due to the fact that surface waters compose a relatively small  
616 amount of water availability across Iran in comparison to other storages such as groundwater.

617 It can also be inferred from Table 4 that removing the water use from scenario (i) results  
618 in smaller canonical correlation in (ii), which means a smaller agreement between variables in  
619 scenario (ii) and water storage changes, even though this removal causes  $\sim 3\%$  and  $5\%$  increase in  
620 loadings of precipitation and temperature, respectively. Comparing the results of both scenarios  
621 implies the large anthropogenic impact (more than climate-related factors) on water storages  
622 variations, which makes it essential to include this impact along with climatic effects while one  
623 studies sub-surface water storage variations in Iran. Figure 16 depicts scatter bi-plots and the  
624 linear trend which represents the correspondence between two sets of variables using average  
625 canonical coefficients for each scenario. It can be seen that the distribution of the two datasets  
626 in scenario (i) has smaller deviations and is more symmetric (closer to the reference line than  
627 scenario (ii)), which leads to higher canonical correlation for the first scenario. Figure 16 shows  
628 that incorporating the water use results in a better agreement between the criterion, i.e., water  
629 storage variations and predicant. This stresses the necessity of considering the water use and  
630 anthropogenic impacts (e.g., irrigation) on water storages analyzes, which cannot be happen  
631 without inclusion of GRACE TWS into the process.

FIGURE 16

## 632 5. Conclusions

633 Sub-surface water storages are a major source of freshwater in Iran. With increased  
634 population and irrigated land, water availability has become a serious issue across the country.  
635 In the present study we assimilate GRACE TWS into W3RA to separately analyze different  
636 water compartments including groundwater, soil moisture, and surface water storages. The  
637 six major drainage divisions in the area including the eastern part of Iran (East), Caspian  
638 Sea, Centre, Sarakhs, Persian Gulf and Oman Sea, and Lake Urmia are considered to better  
639 understand water availability in the different regions. An analysis is undertaken to examine the

640 effects of GRACE data assimilation on different water storage compartments. It is found that  
641 the implemented process can effectively distribute the TWS increments between groundwater  
642 and soil moisture storages. Although the results show improvements in both groundwater and  
643 soil moisture, the data assimilation still may have introduced some artefacts into the simulated  
644 groundwater dynamics due to the massive effects of groundwater extraction within the country,  
645 which requires an independent extensive study and more comprehensive analysis.

646 It is found that the application of GRACE TWS data assimilation can significantly improve  
647 the performance of W3RA. Data assimilation successfully correct for the open-loop simulation  
648 variations, e.g., in terms of trends and multi-year variations, especially for groundwater storage.  
649 Based on the improved estimates, we find that groundwater trends in a large part of the  
650 country's central, western and southern areas are negative representing a significant water  
651 availability issue. An average -8.9 mm/year water storages decline is observed during 2002 to  
652 2012 with a larger rate since 2005 suggesting that Iran is becoming considerably dryer. Larger  
653 water store depletions are found to occur in the Persian Gulf and Oman Sea and Lake Urmia  
654 with lesser effects on soil moisture in these regions. In the Caspian Sea region, however, due to  
655 a large amount of precipitation, smaller groundwater and soil moisture trends are observed. In  
656 the Persian Gulf and Oman Sea, -9.3 mm/year (on average) groundwater trend is found, which  
657 is the second largest negative trend after that of Lake Urmia.

658 Furthermore, PCA is applied to investigate the relationship between the estimated ground-  
659 water and GRACE TWS, as well as their connection to climatic impacts in various parts of  
660 Iran. Larger water storage spatial variations are observed over the northern and western parts  
661 of Iran with higher altitudes in which precipitation rates are generally high. Contrary to rainfall  
662 maps, strong positive GRACE TWS and groundwater signals are found over the north toward  
663 the northwest and partially in western areas. In terms of temporal variations, water storage  
664 variables generally demonstrate the same variation pattern as precipitation, however, they are  
665 also affected by non-climate factors (e.g., anthropogenic impacts), which are likely the cause of  
666 the observed negative trends in GRACE TWS and groundwater time series. Therefore, CCA is  
667 applied to explore the relationship between water storages estimated by data assimilation and  
668 climatic, as well as anthropogenic indicators. The application of CCA reveals strong correla-  
669 tion (0.89 in average) suggesting that the groundwater use has a major impact on water storage  
670 variations.

671 **Acknowledgement**

672 M. Khaki is grateful for the research grant of Curtin International Postgraduate Research  
 673 Scholarships (CIPRS)/ORD Scholarship provided by Curtin University (Australia). This work  
 674 is a TIGeR publication.

675 **References**676 **References**

- 677 Afshar, A.A., Joodaki, G.R., Sharifi, M.A. (2016). Evaluation of Groundwater Resources in  
 678 Iran Using GRACE Gravity Satellite Data. *JGST.*, 5 (4) :73-84, <http://jgst.issge.ir/article-1-381-fa.html>.  
 679
- 680 Amery, H.A., Wolf, A.T. (2000). *Water in the Middle East: A Geography of Peace*, University  
 681 of Texas Press, Austin, Tex.
- 682 Anderson, J. (2001). An Ensemble Adjustment Kalman Filter for Data As-  
 683 simulation. *Mon. Wea. Rev.*, 129, 2884-2903, [http://dx.doi.org/10.1175/1520-0493\(2001\)129;2884:AEAKFF;2.0.CO;2](http://dx.doi.org/10.1175/1520-0493(2001)129;2884:AEAKFF;2.0.CO;2).  
 684
- 685 Anderson, M.C., Norman, J.M., Mecikalski, J.R., Otkin, J.A., Kustas, W.P. (2007). A climato-  
 686 logical study of evapotranspiration and moisture stress across the continental United States  
 687 based on thermal remote sensing: 1. Model formulation. *J. Geophys. Res.* 112 (D10117).  
 688 <http://dx.doi.org/10.1029/2006JD007506>.
- 689 Ardakani, R. (2009). Overview of water management in Iran. *Proceeding of regional center on*  
 690 *urban water management*, Tehran, Iran.
- 691 Bennett, A.F. (2002); *Inverse Modeling of the Ocean and Atmosphere*, 234 pp., Cambridge  
 692 Univ. Press, New York.
- 693 Bertino, L., Evensen G., Wackernagel, H. (2003). Sequential Data Assimilation Techniques in  
 694 Oceanography, *International Statistical Review*, Vol. 71, No. 2, pp. 223-241.
- 695 Chang, B., Kruger, U., Kustra, R., Zhang, J. (2013). Canonical Correlation Analysis based  
 696 on Hilbert-Schmidt Independence Criterion and Centered Kernel Target Alignment, Volume  
 697 28: *Proceedings of The 30th International Conference on Machine Learning*, 2, 28, 316-324,  
 698 <http://jmlr.csail.mit.edu/proceedings/papers/v28/chang13.pdf>.

- 699 Chen, J.L., Wilson, C.R., Famiglietti, J.S., Rodell, M. (2007). Attenuation effect on seasonal  
700 basin-scale water storage changes from GRACE time-variable gravity. *Journal of Geodesy*,  
701 81, 4, 237245. <http://dx.doi.org/10.1007/s00190-006-0104-2>.
- 702 Chen, J.L., Wilson, C.R., Tapley, B.D. (2013). Contribution of ice sheet and mountain glacier  
703 melt to recent sea level rise. *Nat. Geosci.*, 6, 549552, <http://dx.doi.org/10.1038/ngeo1829>.
- 704 Cheng, M.K., Tapley, B.D. (2004). Variations in the Earth's oblateness during  
705 the past 28 years. *Journal of Geophysical Research, Solid Earth*, 109, B09402.  
706 <http://dx.doi.org/10.1029/2004JB003028>.
- 707 Coumou, D., Rahmstorf, S. (2012). A decade of weather extremes *Nat. Clim. Change*, 2 (7),  
708 pp. 16.
- 709 Dattalo, P. (2014). A demonstration of canonical correlation analysis with orthogonal rota-  
710 tion to facilitate interpretation. Unpublished manuscript, School of Social Work, Virginia  
711 Commonwealth University, Richmond, Virginia.
- 712 Döll, P., Kaspar, F., Lehner, B. (2003). A global hydrological model for deriving water avail-  
713 ability indicators: model tuning and validation, *J. Hydrol.*, 270, 105134.
- 714 Eicker, A., Schumacher, M., Kusche, J., Dll, P., Mller-Schmied, H., (2014). Calibration/data  
715 assimilation approach for integrating GRACE data into the WaterGAP global hydrology  
716 model (WGHM) using an ensemble Kalman filter: first results, *SurvGeophys*, 35(6):12851309.  
717 <http://dx.doi.org/10.1007/s10712-014-9309-8>.
- 718 Evensen, G. (2003). The ensemble Kalman filter: Theoretical formulation and practical imple-  
719 mentation, *Ocean Dynamics*, 53, 343367, <http://dx.doi.org/10.1007/s10236-003-0036-9>.
- 720 FAO (Food and Agriculture Organization of the United Nations)(2009). FAO water report, 34.
- 721 Fatolazadeh, F., Voosoghi, B., Naeeni, M.R. (2016). Wavelet and Gaussian Approaches  
722 for Estimation of Groundwater Variations Using GRACE Data. *Groundwater*, 54: 7481,  
723 <http://dx.doi.org/10.1111/gwat.12325>.
- 724 Forootan, E., Rietbroek, R., Kusche, J., Sharifi, M.A., Awange, J., Schmidt, M., Omondi,  
725 P., Famiglietti, J. (2014a). Separation of large scale water storage patterns over Iran using

- 726 GRACE, altimetry and hydrological data. *Journal of Remote Sensing of Environment*, 140,  
727 580-595, <http://doi.org/10.1016/j.rse.2013.09.025>.
- 728 Forootan, E., Didova, O., Schumacher, M., Kusche, J., Elsaka, B. (2014b). Comparisons of  
729 atmospheric mass variations derived from ECMWF reanalysis and operational fields, over  
730 2003 to 2011. *Journal of Geodesy*, 88, Pages 503-514, [http://dx.doi.org/10.1007/s00190-014-](http://dx.doi.org/10.1007/s00190-014-0696-x)  
731 0696-x.
- 732 Forootan, E., Safari, A., Mostafaie, A., Schumacher, M., Delavar, M., Awange, J. (2017).  
733 Large-scale total water storage and water flux changes over the arid and semi-arid  
734 parts of the Middle East from GRACE and reanalysis products. *Surveys in Geophysics*,  
735 <http://dx.doi.org/10.1007/s10712-016-9403-1>.
- 736 Garner, T.W., Wolf, R.A., Spiro, R.W. , Thomsen, M.F. (1999). First attempt at assimilating  
737 data to constrain a magnetospheric model, *J. Geophys. Res.*, 104(A11), 2514525152,  
738 <http://dx.doi.org/10.1029/1999JA900274>.
- 739 Giroto, M., De Lannoy, G.J., Reichle, R.H., Rodell, M. (2016). Assimilation of gridded terres-  
740 trial water storage observations from GRACE into a land surface model. *Water Resources*  
741 *Research*, 52(5), 4164-4183.
- 742 Giroto, M., De Lannoy, G.J., Reichle, R.H., Rodell, M., Draper, C., Bhanja, S.N., Mukherjee,  
743 A. (2017). Benefits and Pitfalls of GRACE Data Assimilation: a Case Study of Terrestrial  
744 Water Storage Depletion in India. *Geophysical Research Letters*.
- 745 Golian, S., Mazdiyasn, O., AghaKouchak, A. (2015). Trends in meteorological and agricultural  
746 droughts in Iran. *Theor Appl Climatol* (2015) 119:679688, [http://dx.doi.org/10.1007/s00704-](http://dx.doi.org/10.1007/s00704-014-1139-6)  
747 014-1139-6.
- 748 Harris, I.C. (2008). Climatic Research Unit (CRU) time-series datasets of variations in  
749 climate with variations in other phenomena. NCAS British Atmospheric Data Cen-  
750 tre, date of citation, University of East Anglia Climatic Research Unit; Jones, P.D.,  
751 <http://catalogue.ceda.ac.uk/uuid/3f894480cc48e1cbc29a5ee12d8542d>.
- 752 Hoteit, I., Pham, D.T., Triantafyllou, G., Korres, G. (2008). A new approximate solution of  
753 the optimal nonlinear filter for data assimilation in meteorology and oceanography, *Monthly*  
754 *Weather Review*, 136, 317-334.

- 755 Hoteit, I., Pham, D.T., Gharamti, M. E., Luo, X. (2015). Mitigating Observation Perturbation  
756 Sampling Errors in the Stochastic EnKF, *Monthly Weather Review*, 143:7, 2918-2936.
- 757 Huntington, T.G. (2006). Evidence for intensification of the global water cycle: Review and  
758 synthesis, *J. Hydrol.*,319(14), 8395, <http://dx.doi.org/10.1016/j.jhydrol.2005.07.003>.
- 759 Joodaki, G., Wahr, J., Swenson, S. (2014). Estimating the human contribution to groundwater  
760 depletion in the Middle East, from GRACE data, land surface models, and well observations,  
761 *Water Resour. Res.*, 50, 26792692, <http://dx.doi.org/10.1002/2013WR014633>.
- 762 Kalnay, E. (2003). Atmospheric modelling, data assimilation and predictability. Cam-  
763 bridge University Press. pp. xxii 341. ISBNs 0 521 79179 0, 0 521 79629 6,  
764 <http://dx.doi.org/10.1256/00359000360683511>.
- 765 Karamouzian, M., Haghdoost, A.K. (2015). Population control policies in Iran, *The*  
766 *Lancet*, Volume 385, Issue 9973, 2127 March 2015, Page 1071, ISSN 0140-6736,  
767 [https://doi.org/10.1016/S0140-6736\(15\)60596-7](https://doi.org/10.1016/S0140-6736(15)60596-7).
- 768 Khaki, M., Forootan, E., Sharifi, M.A. (2014). Satellite radar altimetry wave-  
769 form retracking over the Caspian Sea. *Int. J. Remote Sens.*, 35(17), 63296356,  
770 <http://dx.doi.org/10.1080/01431161.2014.951741>.
- 771 Khaki, M., Forootan, E., Sharifi, M.A., Awange, J., Kuhn, M., (2015). Improved grav-  
772 ity anomaly fields from retracked multimission satellite radar altimetry observations  
773 over the Persian Gulf and the Caspian Sea. *Geophys. J. Int.* 202 (3): 1522-1534,  
774 <http://dx.doi.org/10.1093/gji/ggv240>.
- 775 Khaki, M., Hoteit, I., Kuhn, M., Awange, J., Forootan, E., van Dijk, A.I.J.M., Schumacher,  
776 M., Pattiaratchi, C., (2017a). Assessing sequential data assimilation techniques for integrating  
777 GRACE data into a hydrological model, *Advances in Water Resources*, Volume 107, Pages  
778 301-316, ISSN 0309-1708, <http://dx.doi.org/10.1016/j.advwatres.2017.07.001>.
- 779 Khaki, M., Ait-El-Fquih, B., Hoteit, I., Forootan, E., Awange, J., Kuhn, M., (2017b). A  
780 Two-update Ensemble Kalman Filter for Land Hydrological Data Assimilation with an Un-  
781 certain Constraint, *Journal of Hydrology*, Available online 25 October 2017, ISSN 0022-1694,  
782 <https://doi.org/10.1016/j.jhydrol.2017.10.032>.

- 783 Khaki, M., Schumacher, M., J., Forootan, Kuhn, M., Awange, E., van Dijk, A.I.J.M., (2017c).  
784 Accounting for Spatial Correlation Errors in the Assimilation of GRACE into Hydrological  
785 Models through localization, *Advances in Water Resources*, Available online 1 August 2017,  
786 ISSN 0309-1708, <https://doi.org/10.1016/j.advwatres.2017.07.024>.
- 787 Khaki, M., Forootan, E., Kuhn, M., Awange, J., Papa, F., Shum, C.K., (2018a). A Study of  
788 Bangladesh's Sub-surface Water Storages Using Satellite Products and Data Assimilation  
789 Scheme, *Science of The Total Environment*, Volume 625, 2018, Pages 963-977, ISSN 0048-  
790 9697, <https://doi.org/10.1016/j.scitotenv.2017.12.289>.
- 791 Khaki, M., Forootan, E., Kuhn, M., Awange, J., Longuevergne, L., Wada, W., (2018b). Efficient  
792 Basin Scale Filtering of GRACE Satellite Products, In *Remote Sensing of Environment*,  
793 Volume 204, Pages 76-93, ISSN 0034-4257, <https://doi.org/10.1016/j.rse.2017.10.040>.
- 794 Knapp, T.R. (1978). Canonical correlation analysis: A general parametric significance-testing  
795 system. *Psychological Bulletin*. 85 (2): 410-416. <http://dx.doi.org/10.1037/0033-2909.85.2.410>
- 796 Kusche, J., Schmidt R., Petrovic, S., Rietbroek, R. (2009). Decorrelated GRACE time-variable  
797 gravity solutions by GFZ and their validation using a hydrological model, *Journal of Geodesy*,  
798 DOI 10.1007/s00190-009-0308-3.
- 799 Lahoz, W.A., Geer, A.J., Bekki, S., Bormann, N., Ceccherini, S., Elbern, H., Errera, Q., Eskes,  
800 H.J., Fonteyn, D., Jackson, D.R., Khattatov, B. (2007). The Assimilation of Envisat data  
801 (ASSET) project, *Atmos. Chem. Phys.*, 7, 1773 - 1796.
- 802 Li, B., Rodell, M. (2015). Evaluation of a model-based groundwater drought indicator in the  
803 conterminous US. *Journal of Hydrology*, 526, 78-88.
- 804 Lorenz, E. (1956). Empirical orthogonal function and statistical weather prediction. Technical  
805 Report Science Report No 1, Statistical Forecasting Project. MIT, Cambridge.
- 806 Madani, K. (2014). Water management in Iran: what is causing the looming crisis? *J Environ*  
807 *Stud Sci*. doi:10.1007/s13412-014-0182-z.
- 808 Mayer-Gürr, T., Zehentner, N., Klinger, B., Kvas, A. (2014). ITSG-Grace2014: a new GRACE  
809 gravity field release computed in Graz. - in: GRACE Science Team Meeting (GSTM), Pots-  
810 dam am: 29.09.2014.



- 811 Michel, D. (2017). Iran's impending water crisis. In *Water, Security, and US Policy*, edited by  
812 David Reed. 438 pages, ISBN-10:1138051519.
- 813 Mohammadi-Ghaleni, M., Ebrahimi, K. (2011). Assessing impact of irrigation and drainage  
814 network on surface and groundwater resources Case study: Saveh Plain, Iran, ICID 21st  
815 International Congress on Irrigation and Drainage, 1523 October 2011, Tehran, Iran.
- 816 Motagh, M., Walter, T.R., Sharifi, M.A., Fielding, E., Schenk, A., Anderssohn, J., et al. (2008).  
817 Land subsidence in Iran caused by widespread water reservoir overexploitation. *Geophysical*  
818 *Research Letters*, 35, L16403. <http://dx.doi.org/10.1029/2008GL033814>.
- 819 Müller Schmied, H., S. Eisner, D. Franz, M. Wattenbach, F. Portmann, M. Flrke, and P. Dll  
820 (2014), Sensitivity of simulated global-scale freshwater fluxes and storages to input data,  
821 hydrological model structure, human water use and calibration, *Hydrol. Earth. Syst. Sci.*, 18,  
822 35113538, <http://dx.doi.org/10.5194/hess-18-3511-2014>.
- 823 Munier, S., Aires, F., Schlaffe, S., Prigent, C., Papa, F., Maisongrande, P., Pan, M. (2014).  
824 Combining data sets of satellite-retrieved products for basin-scale water balance study: 2.  
825 Evaluation on the Mississippi Basin and closure correction model. *Journal of Geophysical*  
826 *Research: Atmospheres*, 119, 12,100-12,116, <http://dx.doi.org/10.1002/2014JD021953>.
- 827 Njoku, E.G. et al. (2003). Soil moisture retrieval from AMSR-e. *IEEE Transactions on Geo-*  
828 *science and Remote Sensing*. 41:2, 215-229.
- 829 Ott, E., Hunt, B.R., Szunyogh, I., Zimin, A.V., Kostelich, E.J., Corazza, M., Kalnay, E., Patil,  
830 D.J., Yorke, J.A. (2004). A local ensemble Kalman Filter for atmospheric data assimilation.  
831 *Tellus*, 56A: 415-428.
- 832 Oke, P.R., Brassington, G.B., Griffin, D.A., Schiller, A. (2008). The Bluelink Ocean  
833 Data Assimilation System (BODAS). *Ocean Modelling*, 21, 4670, [http://dx.doi.org/](http://dx.doi.org/10.1016/j.ocemod.2007.11.002)  
834 [10.1016/j.ocemod.2007.11.002](http://dx.doi.org/10.1016/j.ocemod.2007.11.002).
- 835 Reager, J.T., Thomas, A.C., Sproles, E.A., Rodell, M., Beaudoin, H.K., Li, B., Famiglietti, J.S.  
836 (2015). Assimilation of GRACE Terrestrial Water Storage Observations into a Land Surface  
837 Model for the Assessment of Regional Flood Potential. *Remote Sens.* 2015, 7, 14663-14679.
- 838 Renzullo, L.J., Van Dijk, A.I.J.M., Perraud, J.M., Collins, D., Henderson, B., Jin, H., Smith,  
839 A.B., McJannet, D.L. (2014). Continental satellite soil moisture data assimilation improves

- 840 root-zone moisture analysis for water resources assessment. *J. Hydrol.*, 519, 27472762.  
841 <http://dx.doi.org/10.1016/j.jhydrol.2014.08.008>.
- 842 Rodell, M., Houser, P. R., Jambor, U., Gottschalck, J., Mitchell, K., Meng, C. J., Arsenault,  
843 K., Cosgrove, B., Radakovich, J., Bosilovich, M., Entin, J. K., Walker, J. P., Lohmann, D.,  
844 Toll, D. (2004). The global land data assimilation system. *American Meteorological Society*,  
845 85, 3, 381-394. <http://dx.doi.org/10.1175/BAMS-85-3-381>.
- 846 Sarraf, M., Owaygen, M., Ruta, G., Croitoru, L. (2005). Islamic Republic of Iran: Cost assess-  
847 ment of environmental degradation. Tech. Rep. 32043-IR. Washington, D.C.: World Bank.
- 848 Schmidt, R., Petrovic, S., Gntner, A., Barthelmes, F., Wnsch, J., Kusche, J. (2008). Periodic  
849 components of water storage changes from GRACE and global hydrology models. *J. Geophys.*  
850 *Res.*, 113, B08419, <http://dx.doi.org/10.1029/2007JB005363>.
- 851 Schumacher, M., Kusche, J., Döll, P. (2016). A systematic impact assessment of GRACE  
852 error correlation on data assimilation in hydrological models, *Journal of Geodesy*,  
853 <http://dx.doi.org/10.1007/s00190-016-0892-y>.
- 854 Schumacher, M., Forootan, E., van Dijk, A.I.J.M., Mller Schmied, H., Crosbie, R.S., Kusche,  
855 J., Dll, P. (2018). Improving drought simulations within the Murray-Darling Basin by  
856 combined calibration/assimilation of GRACE data into the WaterGAP Global Hydrology  
857 Model, *Remote Sensing of Environment*, Volume 204, 2018, Pages 212-228, ISSN 0034-4257,  
858 <https://doi.org/10.1016/j.rse.2017.10.029>.
- 859 Schunk, R.W., Scherliess, L., Sojka, J.J., Thompson, D.C. (2004). USU global ionospheric data  
860 assimilation models, *Atmospheric and Environmental Remote Sensing Data Processing and*  
861 *Utilization: an End-to-End System Perspective*, (ed. H.-L. A. Huang and H. J. Bloom), *Proc.*  
862 *of SPIE*, 5548, <http://dx.doi.org/10.1117/12.562448>, 327-336.
- 863 Sheffield, J., Goteti, G., Wood, E.F. (2006). Development of a 50-yearhigh-resolution global  
864 dataset of meteorological forcings for land surfacemodeling, *J. Clim.*, 19(13), 30883111.
- 865 Steiger, J.H., Browne, M.W. (1984). The comparison of interdependent correlations between  
866 optimal linear composites. *Psychometrika*, 49, 1121.
- 867 Stewart, L.M., Dance, S.L., Nichols, N.K. (2008). Correlated observation errors in data assim-  
868 ilation. *Int. J. Numer. Meth. Fluids*, 56: 15211527. <http://dx.doi.org/10.1002/flid.1636>.

- 869 Swenson, S., Chambers, D., Wahr, J. (2008). Estimating geocentervariations from a combi-  
870 nation of GRACE and ocean model output. *Journal of Geophysical research*, 113, B08410,  
871 <http://dx.doi.org/10.1029/2007JB005338>.
- 872 Tangdamrongsub, N., Steele-Dunne, S.C., Gunter, B.C., Ditmar, P.G., and Weerts, A.H.  
873 (2015). Data assimilation of GRACE terrestrial water storage estimates into a regional  
874 hydrological model of the Rhine River basin, *Hydrol. Earth Syst. Sci.*, 19, 2079-2100,  
875 <http://dx.doi.org/10.5194/hess-19-2079-2015>.
- 876 Tapley, B.D., Bettadpur, S., Watkins, M., Reigber, C. (2004). The gravity recovery and climate  
877 experiment: mission overview and early results, *Geophysical Research Letters*, 31, L09607,  
878 doi: 10.1029/2004GL019920.
- 879 Tippett, M.K., Anderson, J.L., Bishop, C.H., Hamill, T.M., Whitaker, J.S. (2003). Ensemble  
880 square root filters, *Mon. Weath. Rev.*, 131, 148590.
- 881 Tourian, M.J., Elmi, O., Chen, Q., Devaraju, B., Roohi, Sh., Sneeuw, N. (2015). A space-  
882 borne multisensor approach to monitor the desiccation of Lake Urmia in Iran, *Remote*  
883 *Sensing of Environment*, Volume 156, January 2015, Pages 349-360, ISSN 0034-4257,  
884 <https://doi.org/10.1016/j.rse.2014.10.006>.
- 885 Tregoning, P., McClusky, S., van Dijk, A.I.J.M., Crosbie, R.S., Pea-Arancibia, J.L. (2012).  
886 Assessment of GRACE satellites for groundwater estimation in Australia, *Waterlines report*,  
887 National Water Commission, Canberra.
- 888 Trigo, R.M., Gouveia, C.M., Barriopedro, D. (2010). The intense 20072009 drought in the  
889 Fertile Crescent: Impact and associated atmospheric circulation, *Agric. For. Meteorol.*, 150,  
890 12451257.
- 891 Tropical Rainfall Measuring Mission (TRMM), (2011). TRMM (TMPA/3B43) Rainfall Es-  
892 timate L3 1 month 0.25 degree x 0.25 degree V7, Greenbelt, MD, Goddard Earth Sci-  
893 ences Data and Information Services Center (GES DISC), Accessed [Data Access Date]  
894 [https://disc.gsfc.nasa.gov/datacollection/TRMM\\_3B43\\_7.html](https://disc.gsfc.nasa.gov/datacollection/TRMM_3B43_7.html).
- 895 United Nations (2015). United Nations Department of Economic and Social Affairs. World  
896 Population Prospects: The 2015 Revision.

- 897 Van Camp, M., Radfar, M., Martens, K., Walraevens, K. (2012). Analysis of the groundwater  
898 resource decline in an intramountain aquifer system in Central Iran. *Geologica Belgica*, 15/3,  
899 176180.
- 900 van Dijk, A.I.J.M. (2010). The Australian Water Resources Assessment System: Technical  
901 Report 3, Landscape model (version 0.5) Technical Description, CSIRO: Water for a Healthy  
902 Country National Research Flagship.
- 903 van Dijk, A.I.J.M., Renzullo, L.J., and Rodell, M. (2011). Use of Gravity Recovery and  
904 Climate Experiment terrestrial water storage retrievals to evaluate model estimates by  
905 the Australian water resources assessment system, *Water Resour. Res.*, 47, W11524,  
906 <http://dx.doi.org/10.1029/2011WR010714>.
- 907 van Dijk, A.I.J.M., Pea-Arancibia, J.L., Wood, E.F., Sheffield, J., Beck, H.E. (2013). Global  
908 analysis of seasonal streamflow predictability using an ensemble prediction system and  
909 observations from 6192 small catchments worldwide, *Water Resour. Res.*, 49, 27292746,  
910 <http://dx.doi.org/10.1002/wrcr.20251>.
- 911 van Dijk, A.I.J.M., Renzullo, L.J., Wada, Y., Tregoning, P. (2014). A global water cycle reanal-  
912 ysis (2003-2012) merging satellite gravimetry and altimetry observations with a hydrological  
913 multi-model ensemble. *Hydrol Earth Syst Sci* 18:29552973, [http://dx.doi.org/10.5194/hess-](http://dx.doi.org/10.5194/hess-18-2955-2014)  
914 18-2955-2014.
- 915 Voss, K.A., Famiglietti, J.S., Lo, M.-H., de Linage, C., Rodell, M., Swenson, S.C. (2013).  
916 Groundwater depletion in the Middle East from GRACE with implications for transboundary  
917 water management in the TigrisEuphratesWestern Iran region. *Water Resources Research*,  
918 49, <http://dx.doi.org/10.1002/wrcr.20078>.
- 919 Vrugt, J.A., ter Braak, C.J.F., Diks, C.G.H., Schoups, G. (2013). Advancing hydrologic data  
920 assimilation using particle Markov chain Monte Carlo simulation: theory, concepts and  
921 applications, *Advances in Water Resources*, Anniversary Issue - 35 Years, 51, 457-478,  
922 <http://dx.doi.org/10.1016/j.advwatres.2012.04.002>.
- 923 Wahr, J.M., Molenaar, M., Bryan, F. (1998). Time variability of the Earth's gravity field:  
924 hydrological and oceanic effects and their possible detection using GRACE. *J Geophys Res*  
925 108(B12):3020530229, <http://dx.doi.org/10.1029/98JB02844>.

- 926 Whitaker, J.S., Hamill, T.M. (2002). Ensemble data assimilation without perturbed observa-  
927 tions, *Mon. Wea. Rev.*, 130, 1913-1924.
- 928 Wolf, A.T., Newton, J.T. (2007). Case study transboundary dispute resolution: The Tigris-  
929 Euphrates Basin, Transboundary Freshwater Dispute Database (TFDD), Oregon State Uni-  
930 versity, <http://www.transboundarywaters.orst.edu/>.
- 931 Zaitchik, B.F., Rodell, M., Reichle, R.H. (2008). Assimilation of GRACE terrestrial water stor-  
932 age data into a land surface model: results for the Mississippi River Basin. *J Hydrometeorol*  
933 9(3):535-548, <http://dx.doi.org/10.1175/2007JHM951.1>.

ACCEPTED MANUSCRIPT

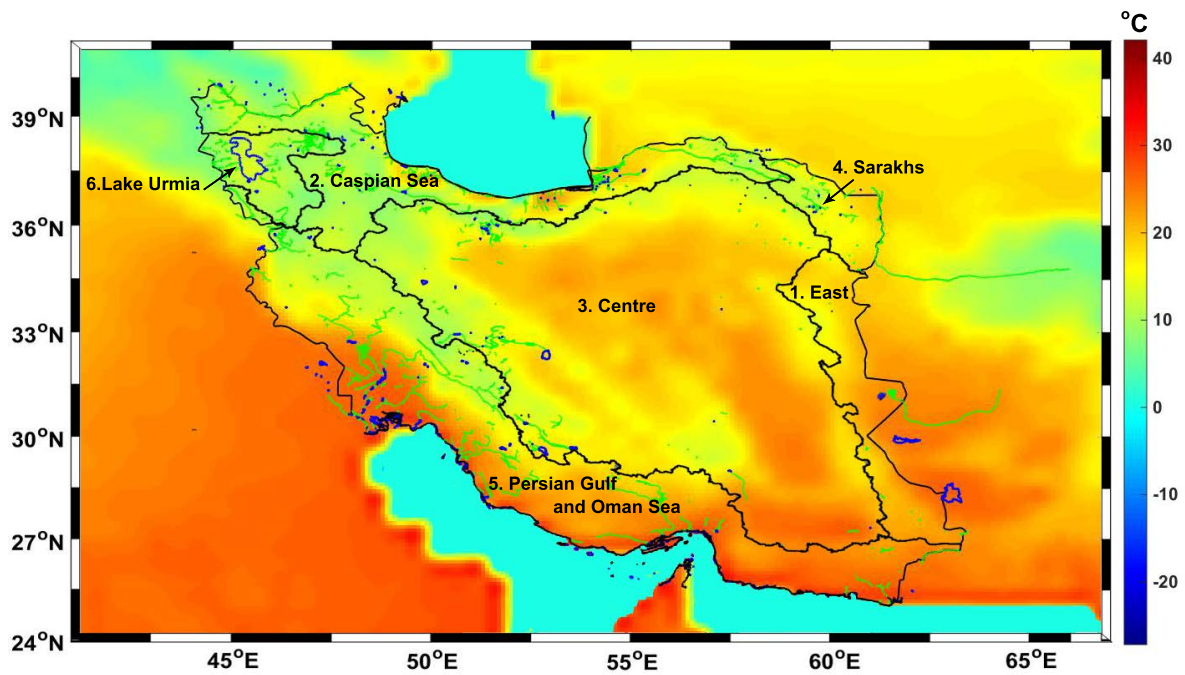


Figure 1: The study area and its average temperature (Harris, 2008). The figure also contains the locations of 6 major catchments separated by black solid lines.

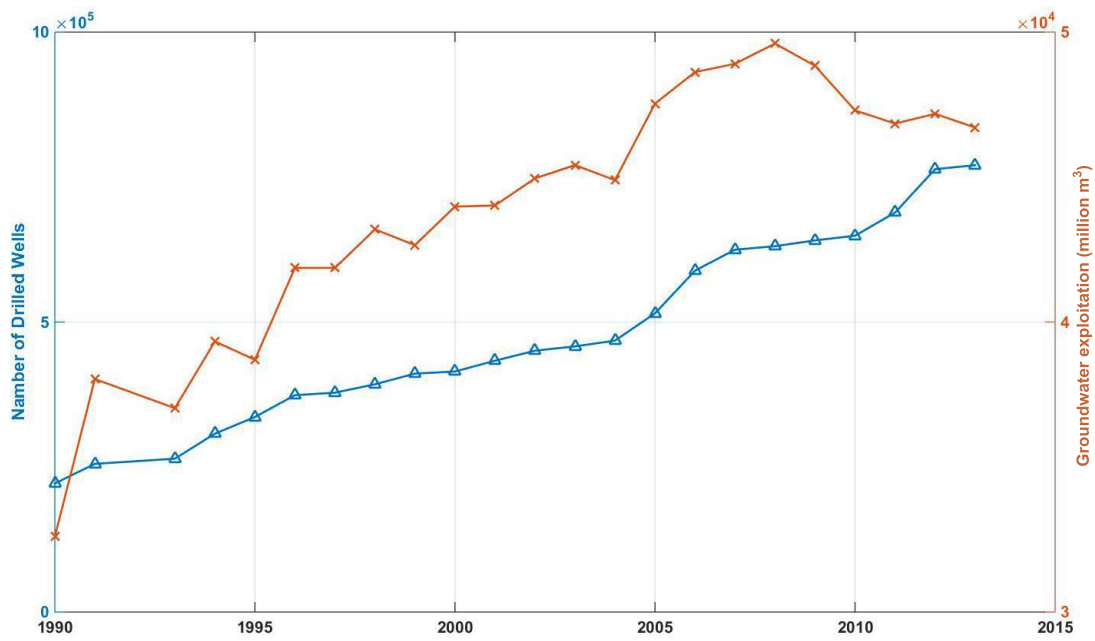


Figure 2: Groundwater depletion and the number of drilled wells in Iran from IWRMC.

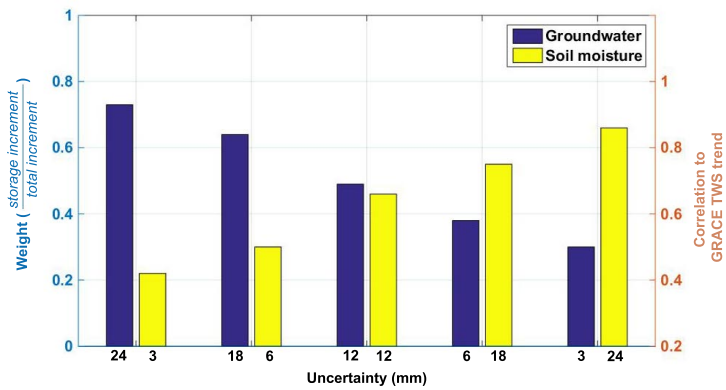


Figure 3: Relationships between groundwater and soil moisture state variable uncertainties and corresponding weights during data assimilation.



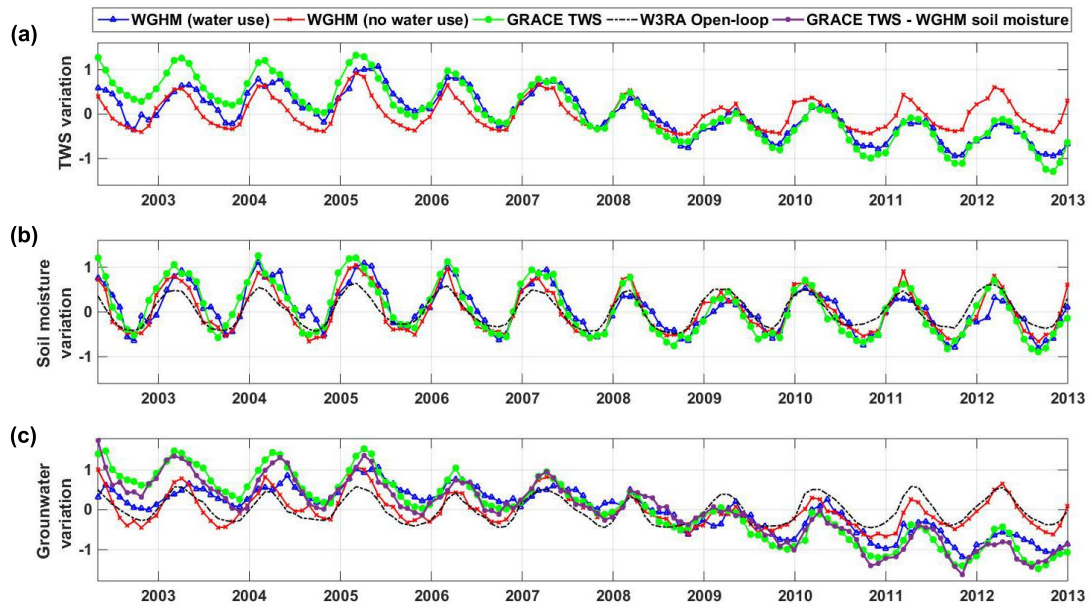


Figure 4: (a) Simulated average TWS observations using WGHM with and without human use, and W3RA open-loop plus GRACE trend. Average soil moisture (b) and groundwater (c) estimates from data assimilation based on simulated observations in (a).

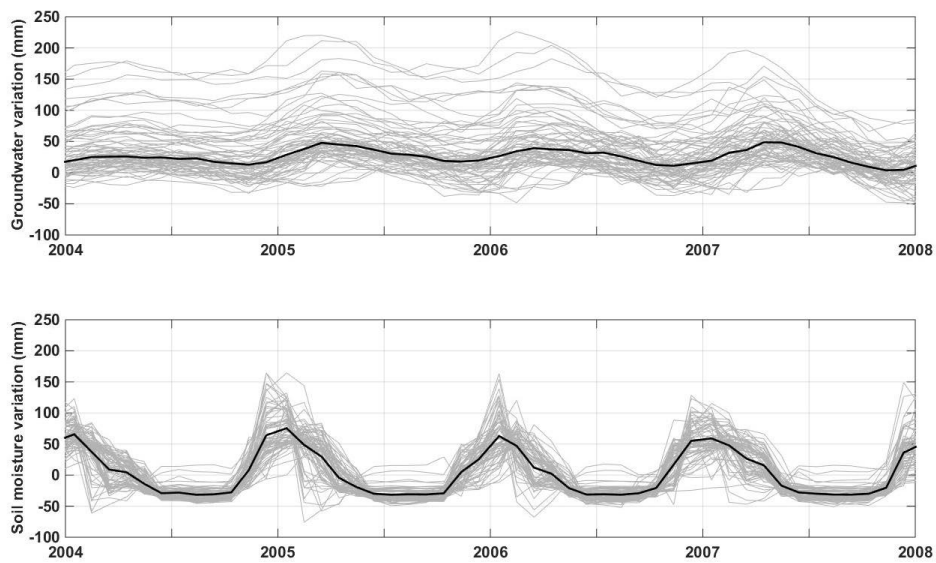


Figure 5: Average groundwater and soil moisture ensemble spreads between 2004 and 2008 over Iran. Gray lines indicate ensemble members and the black solid line present ensemble mean. Larger ensemble propagation is evident compared to that of soil moisture that represents larger uncertainties in the former water storage compartment.

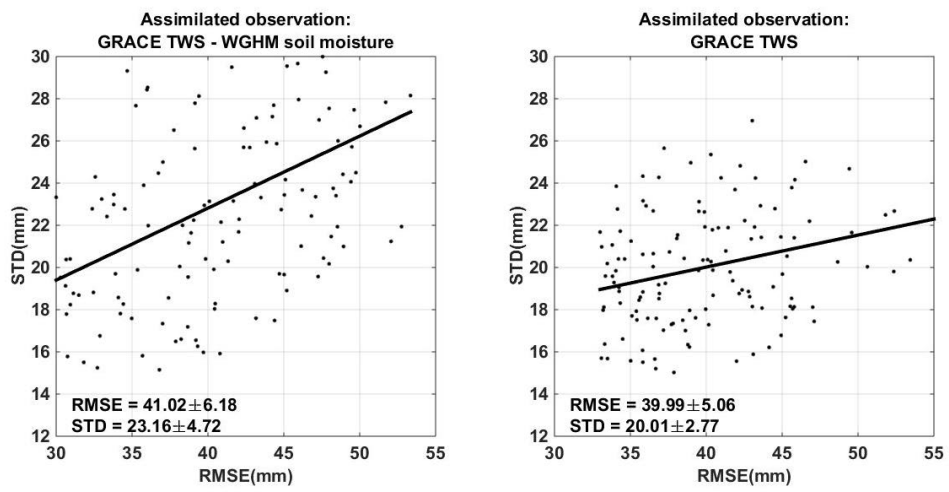


Figure 6: Average groundwater RMSE and STD from assimilating GRACE TWS and GRACE TWS minus soil moisture.

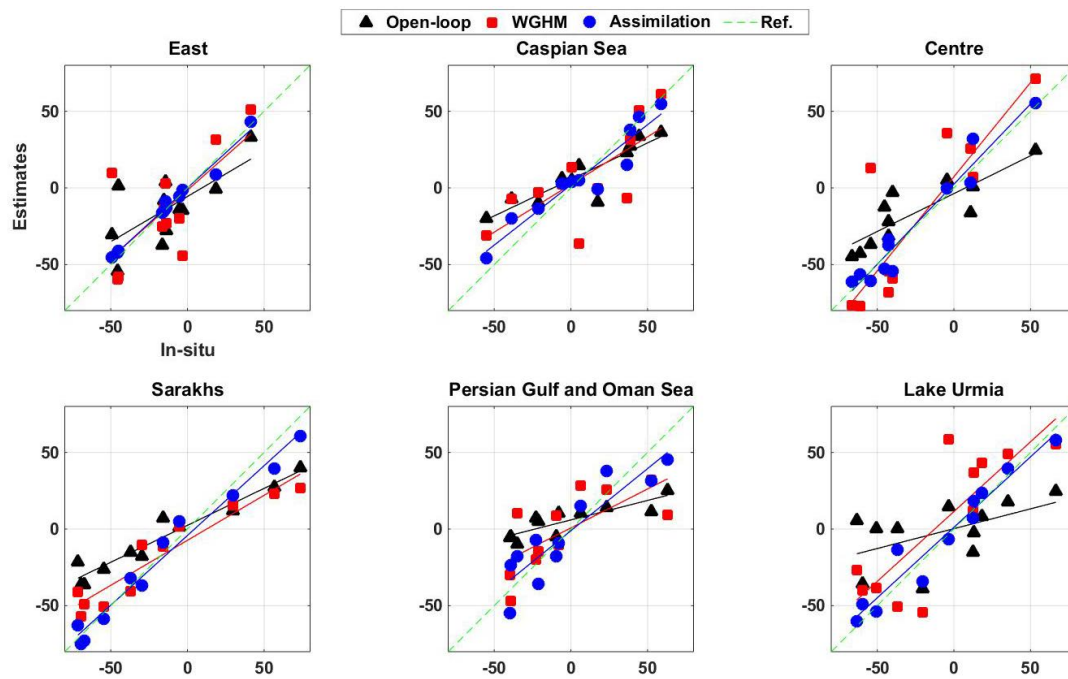


Figure 7: Comparison between in-situ groundwater measurements and those estimated by open-loop run, data assimilation, and WGHM over different catchments (units are mm).

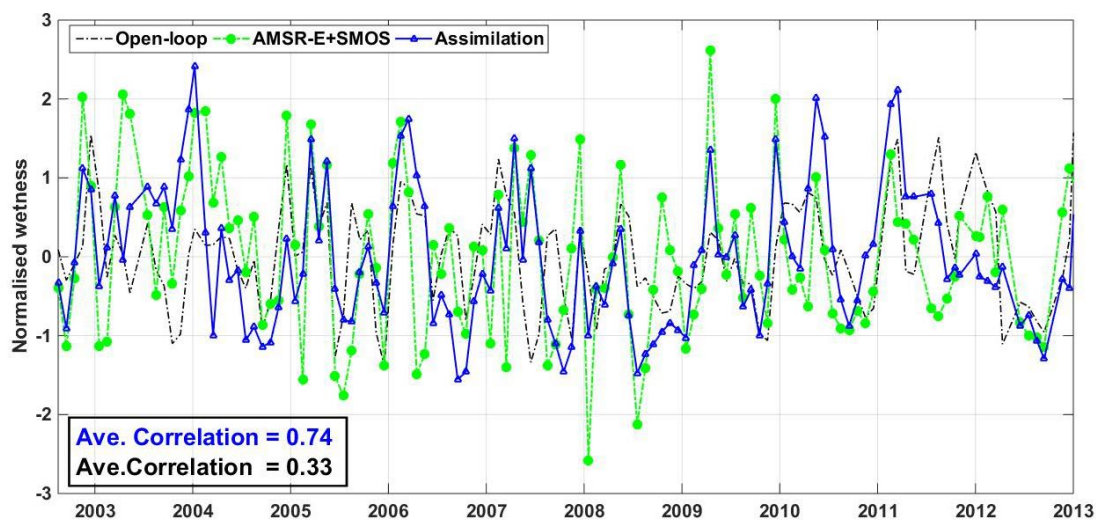


Figure 8: Comparison between the average estimated top layer soil moisture with and without (open-loop) data assimilation and soil moisture observations from satellite remote sensing (AMSR-E+SMOS). Correlations between the satellite measurements and both open-loop and assimilation estimates are also reported in the figure.

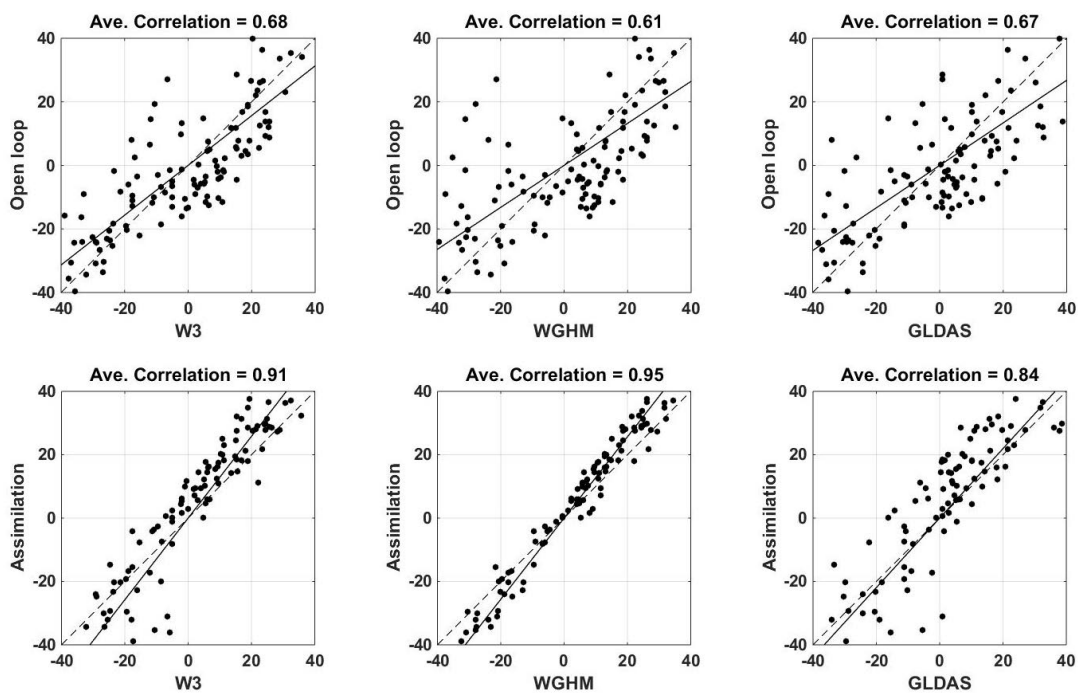


Figure 9: Comparison between the average soil moisture estimates from open-loop and data assimilation, and soil moisture products of W3, WGHM, and GLDAS (units are mm).

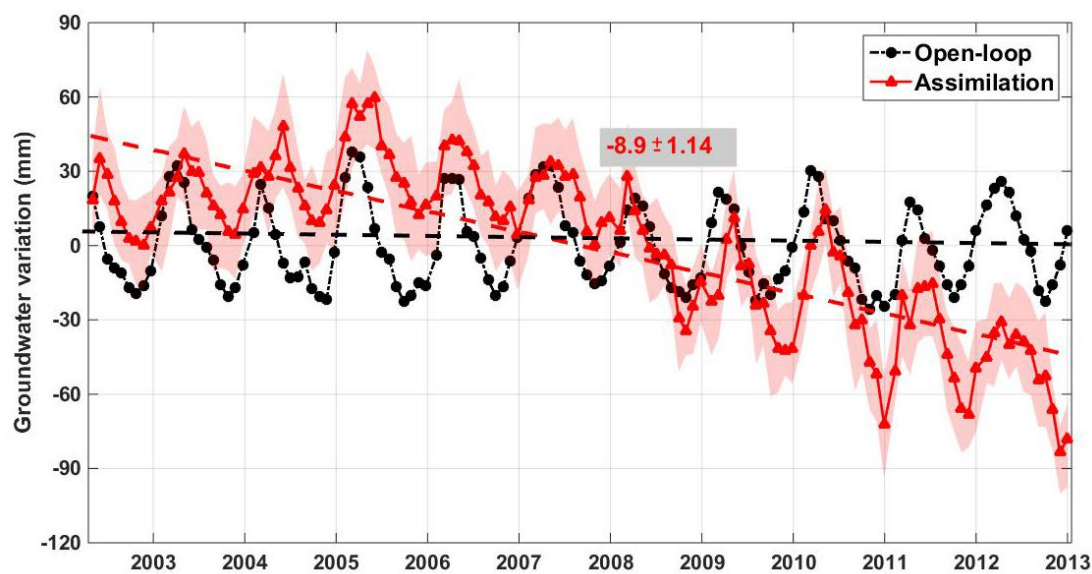


Figure 10: Average groundwater variations within Iran from open-loop and data assimilation results and corresponding 95% confidence intervals (shaded blue). Trend lines for time series are also displayed by dashed lines. Note that the open-loop time series slope is not reported because no significant trend is observed.

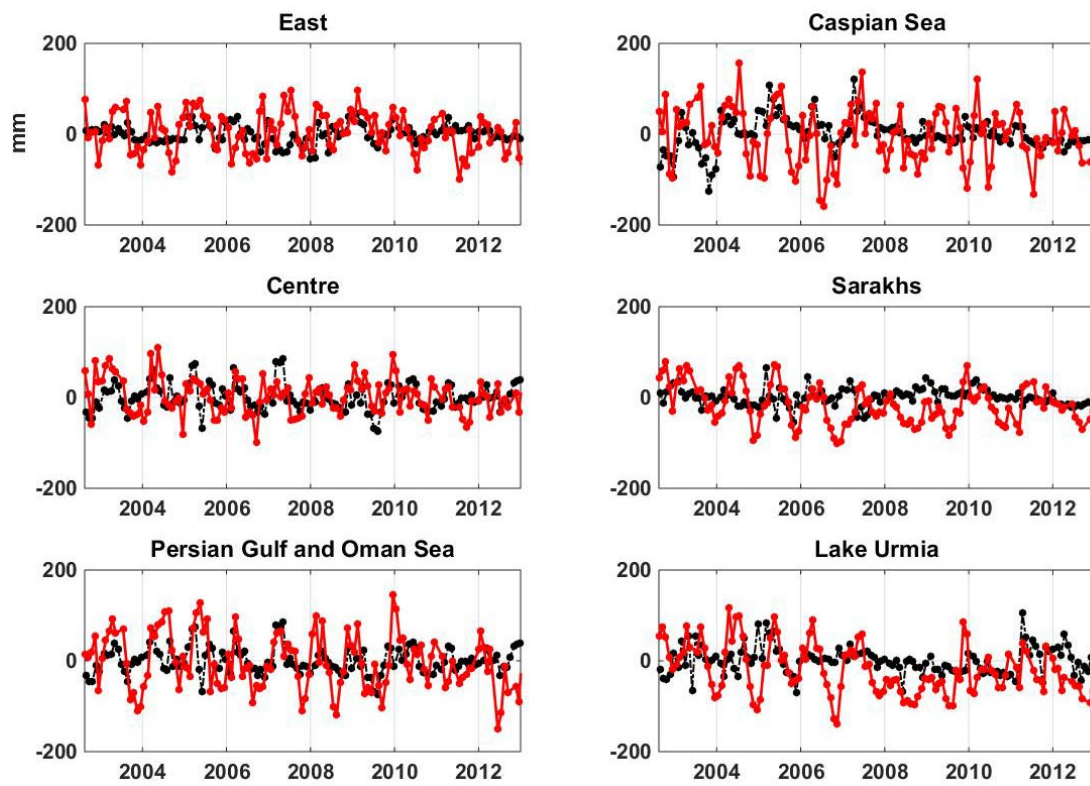


Figure 11: Average time series of soil moisture variations over different catchments with (blue) and without (black) data assimilation.



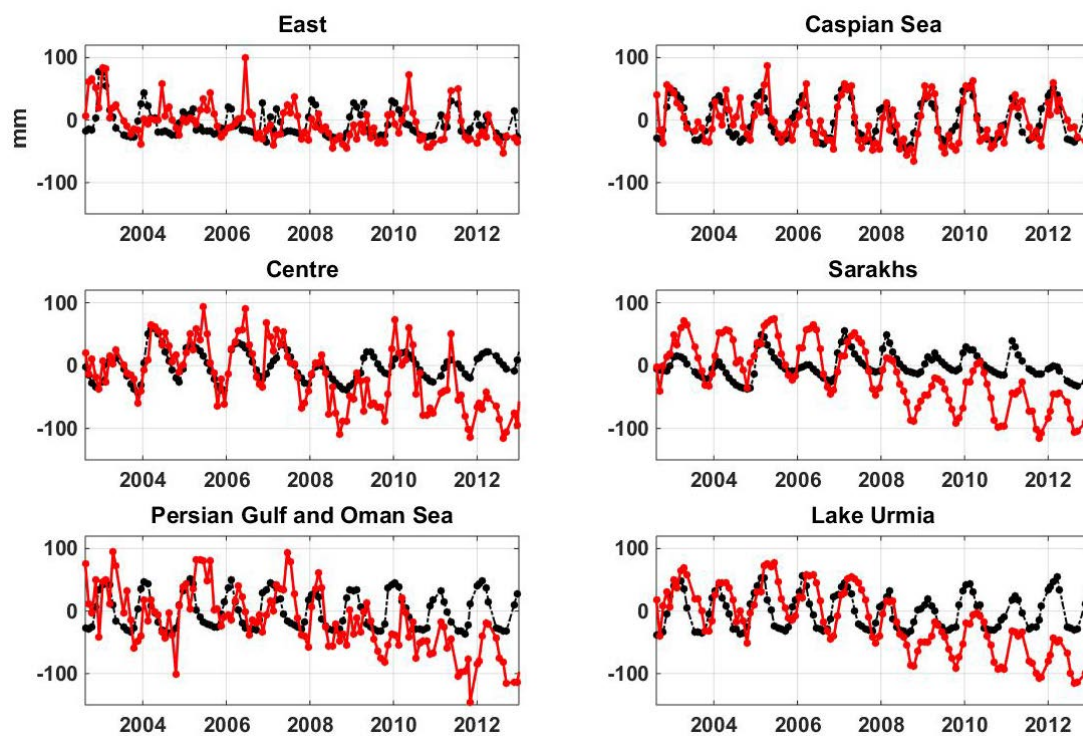


Figure 12: Average time series of groundwater variations over different catchments with (blue) and without (black) data assimilation. The correlations of time series with the in-situ measurements, as well as the trends of assimilation results are reported in Table 2.

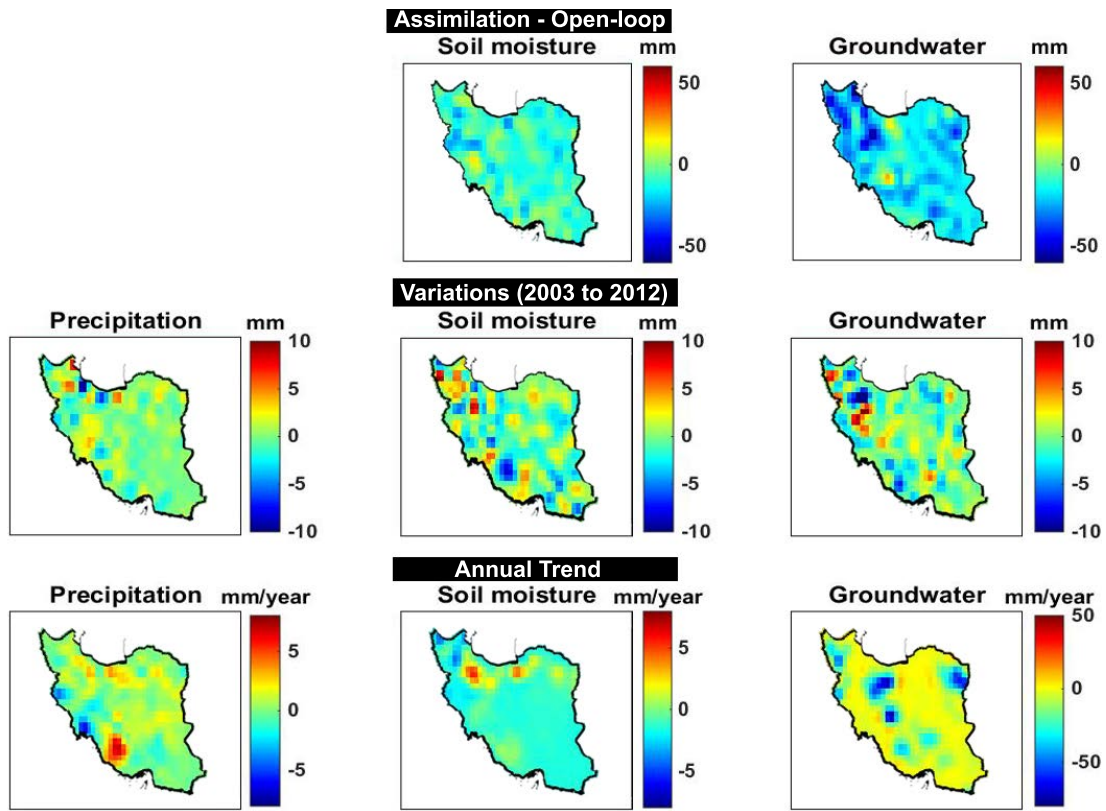


Figure 13: First row: temporally averaged increments applied to soil moisture and groundwater storages. Second row: variation of precipitation, soil moisture, and groundwater (after data assimilation) estimated as the average of each time series at each grid point. Third row: gridded trend of time series precipitation, soil moisture, and groundwater (after data assimilation) time series.

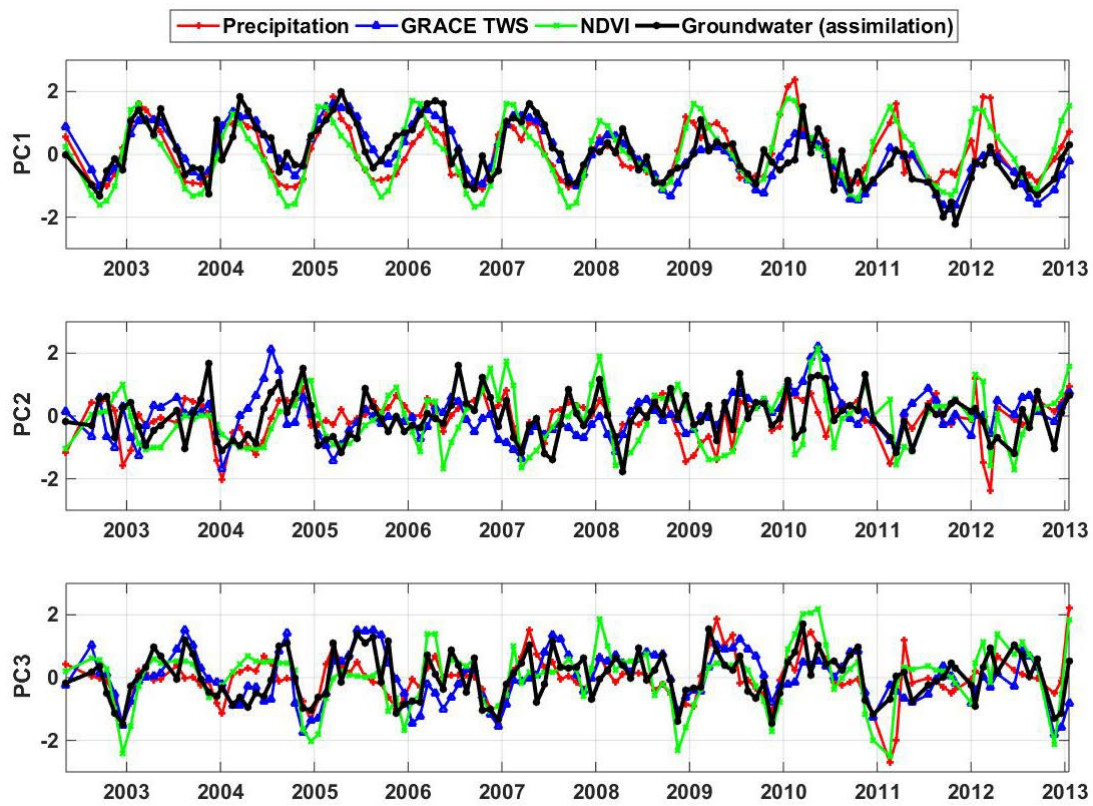


Figure 14: The three first principal components of precipitation, GRACE TWS, NDVI, and groundwater.

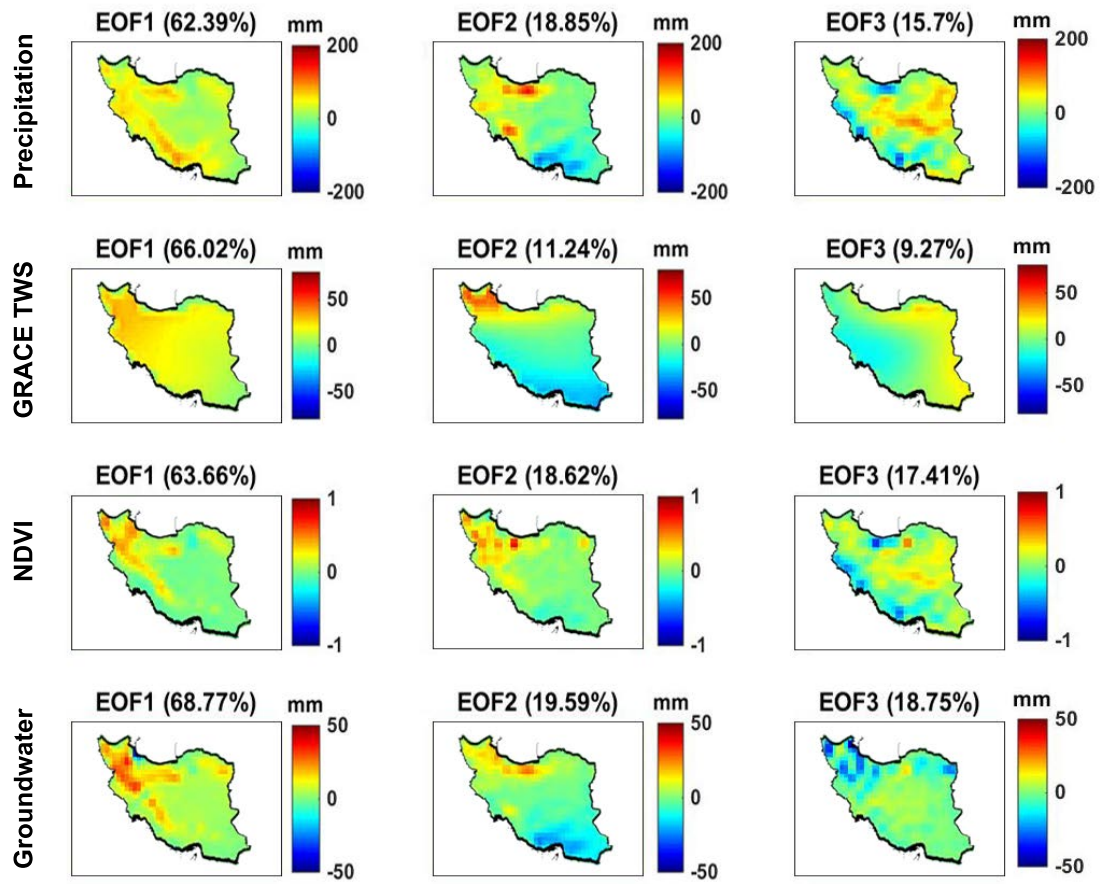


Figure 15: The empirical orthogonal functions (EOF1, EOF2, and EOF3) extracted from precipitation, GRACE TWS, NDVI, and groundwater.

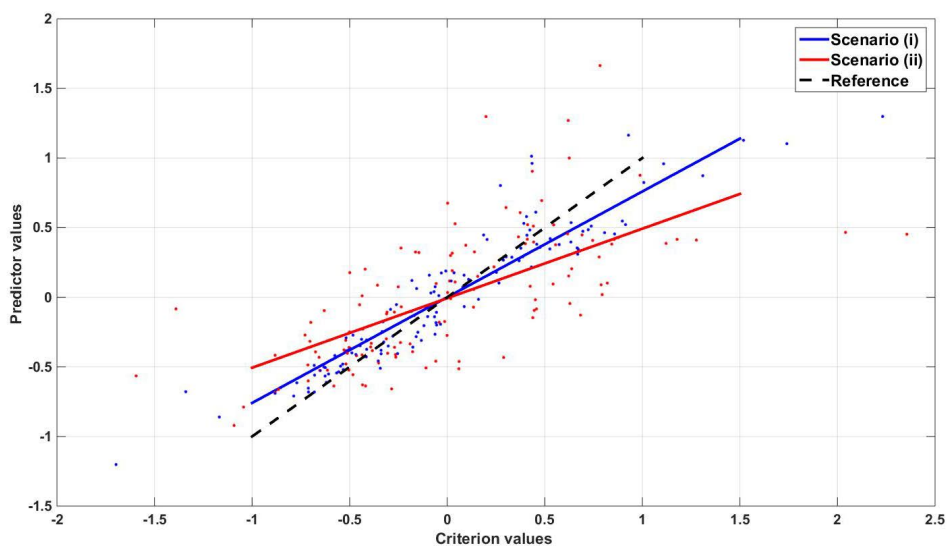


Figure 16: Scatter bi-plots (circles) and the linear trend (solid lines) of average canonical coefficients from CCA for each scenario applied. The combination of the water storages and discharge data and their canonical coefficients are in the x-axis (as criterion variables), the y-axis represents the combination of the predictor variables. Black solid line represents the reference line.

Table 1: A summary of the datasets used in this study.

| Description                                   | Platform      | Data access   |
|---|---------------|---|
| Terrestrial water storage (TWS)               | GRACE         | <a href="https://www.tugraz.at/institute/ifg/downloads/gravity-field-models/itsg-grace2014/">https://www.tugraz.at/institute/ifg/downloads/gravity-field-models/itsg-grace2014/</a> |
| Precipitation                                 | TRMM-3B43     | <a href="https://disc.gsfc.nasa.gov/datacollection/TRMM_3B43_7.html">https://disc.gsfc.nasa.gov/datacollection/TRMM_3B43_7.html</a>   |
| Normalized Difference Vegetation Index (NDVI) | NASA-GSFC     | <a href="ftp://eclipse.ncdc.noaa.gov/pub/cdr/avhrr-land/ndvi/">ftp://eclipse.ncdc.noaa.gov/pub/cdr/avhrr-land/ndvi/</a>   |
| Hydrological model                            | W3RA          | <a href="http://www.wenfo.org/wald/data-software/">http://www.wenfo.org/wald/data-software/</a>   |
| Temperature                                   | Harris (2008) | <a href="https://crudata.uea.ac.uk/cru/data/hrg/">https://crudata.uea.ac.uk/cru/data/hrg/</a>   |
| Groundwater in-situ measurements              | IWRMC         | <a href="http://www.wrm.ir/">http://www.wrm.ir/</a>   |
| Average water consumption                     | IWRMC         | <a href="http://www.wrm.ir/">http://www.wrm.ir/</a>   |
| Discharge data                                | IWRMC         | <a href="http://www.wrm.ir/">http://www.wrm.ir/</a>   |
| Number of groundwater bore holes              | IWRMC         | <a href="http://www.wrm.ir/">http://www.wrm.ir/</a>   |
| Altimetry-derived level height                | Jason-1       | <a href="http://podaac.jpl.nasa.gov">http://podaac.jpl.nasa.gov</a>   |
| Altimetry-derived level height                | Jason-2       | <a href="http://avisoftp.cnes.fr/">http://avisoftp.cnes.fr/</a>   |

Table 2: The undertaken experiments and corresponding research objectives. The result section associated to each experiment is also presented.

| Experiment                 | Research objective  | Result section |
|----------------------------|---|----------------|
| Simulated assimilation     | To assess the impacts of GRACE observations on different water storage                            | Section 4.1    |
| Evaluation procedure       | To examine the validity of results against independent observations                               | Section 4.2    |
| Water storage analysis     | To analyze spatio-temporal variations of groundwater and soil moisture                            | Section 4.3    |
| Climatic impacts using PCA | To investigate the impacts of climate indicators (e.g., precipitation) on water storage           | Section 4.4    |
| CCA                        | To establish the relations between water storages and human- as well as climate-related variables | Section 4.5    |

Table 3: Statistics of groundwater variations and its errors with respect to the in-situ observations. For each region the RMSE average and its range ( $\pm XX$ ) at the 95% confidence interval is presented. Improvements in data assimilation results are calculated for each catchment in relation to the water storages from the model without implementing data assimilation.

| Region                    | Groundwater trend (mm/year) | Assessment with In-situ |               |              |               | Improvement (%) |
|---------------------------|-----------------------------|-------------------------|---------------|--------------|---------------|-----------------|
|                           |                             | Open-loop               |               | Assimilation |               |                 |
|                           |                             | Correlation             | RMSE (mm)     | Correlation  | RMSE (mm)     |                 |
| East                      | -3.8                        | 0.57                    | 60 $\pm$ 8.66 | 0.84         | 38 $\pm$ 4.64 | 36.29           |
| Caspian Sea               | -2.1                        | 0.64                    | 64 $\pm$ 9.19 | 0.73         | 46 $\pm$ 5.13 | 28.13           |
| Centre                    | -6.7                        | 0.63                    | 55 $\pm$ 7.84 | 0.65         | 41 $\pm$ 5.01 | 26.55           |
| Sarakhs                   | -5.4                        | 0.61                    | 52 $\pm$ 7.58 | 0.82         | 32 $\pm$ 4.26 | 38.64           |
| Persian Gulf and Oman Sea | -9.3                        | 0.56                    | 79 $\pm$ 9.07 | 0.75         | 49 $\pm$ 5.17 | 37.81           |
| Lake Urmia                | -11.8                       | 0.52                    | 69 $\pm$ 8.28 | 0.81         | 40 $\pm$ 4.25 | 41.90           |



Table 4: Average canonical correlation coefficients and variable loadings for the data inputs in CCA for each scenario.

|                                   |                          | Scenario (i)           | Scenario (ii)          |
|-----------------------------------|--------------------------|------------------------|------------------------|
|                                   |                          | Canonical coefficients | Canonical coefficients |
| Canonical correlation coefficient |                          | 0.972                  | 0.841                  |
| Predictor variables               | Precipitation            | 0.721                  | 0.749                  |
|                                   | NDVI                     | 0.365                  | 0.412                  |
|                                   | Temperature              | -0.591                 | -0.681                 |
|                                   | Water use for: # Farming | -0.938                 | -                      |
|                                   | # Industry               | -0.758                 | -                      |
|                                   | # Drink (Urban use)      | -0.820                 | -                      |
|                                   | Number of bore holes     | -0.893                 | -                      |
| Criterion variables               | Groundwater              | 0.938                  | 0.705                  |
|                                   | Soil moisture            | 0.633                  | 0.617                  |
|                                   | Water discharge          | 0.174                  | 0.249                  |